Feasibility and accuracy of Received Signal Strength-based Multilateration for aircraft localization using crowdsourced data

MSc Thesis Report

Veronika Martjanova

Delft University of Technology

This page intentionally left blank.

Feasibility and accuracy of Received Signal Strength-based Multilateration for aircraft localization using crowdsourced data

MSc Thesis Report

by

Veronika Martjanova

In fulfilment of the requirements for the MSc degree in Aerospace Engineering
at Delft University of Technology

Student number:	4972759
Supervisor:	Dr. J.Sun
Chair:	Prof.dr.ir. J.M.Hoekstra
Date:	March 25th, 2024
Institution:	Delft University of Technology, Faculty of Aerospace Engineering

An electronic version of this thesis is available at `http://repository.tudelft.nl/`.
Cover image: Photo by Yevhenii Dubrovskyi.

This page intentionally left blank.

Contents

I

Scientific paper

This page intentionally left blank.

Feasibility and accuracy of Received Signal Strength-based Multilateration for aircraft localization using crowdsourced data

Author: V. Martjanova
Supervisors: Dr. J. Sun, Prof. Dr. Ir. J.M. Hoekstra
Control & Simulation, Faculty of Aerospace Engineering
Delft University of Technology, Delft, The Netherlands

***Abstract* - To verify the aircraft position provided by Automatic Dependent Surveillance-Broadcast (ADS-B) transponders, multilateration (MLAT) technique incorporates time difference of arrival (TDOA) measurements at multiple ground-based receivers to estimate the corresponding distances between those and the aircraft. This approach requires precise time synchronization among receivers that can not always be guaranteed. Alternatively, received signal strength (RSS) measurements can be utilized to derive these distances. In this paper, crowdsourced RSS measurements from 43 receivers were used to construct parameterized signal propagation models that capture the relationship between RSS and distance. The quality of these models was evaluated by examination of model parameter and estimated distance errors in both 2D and 3D. The results show that at most 26.3% of available RSS measurements could be represented by the models given the cut-off criteria for model parameter errors. Moreover, the models with higher parameter errors demonstrated poor ability to capture RSS measurements at greater distances. The localization errors in MLAT with TDOA were compared to MLAT with RSS where the later resulted in more accurate position estimation in cases where the receiver clocks were not synchronized. However, MLAT with TDOA generally produced significantly more accurate position estimation given the reliable timestamps of signal arrival. The assessment of localization accuracy using crowdsourced data resulted in root mean square errors of 118.1 meters in MLAT with TDOA and 9858.6 meters in MLAT with RSS in 2D, representing the best results obtained.**

I. INTRODUCTION

In the recent years, a significant shift in air traffic surveillance methods occurred through the integration of Automatic Dependent Surveillance-Broadcast (ADS-B) as an enhancement of traditional radar systems [1]. ADS-B employs an onboard transponder to broadcast real-time information about aircraft position without the need for interrogation from the ground. This technology enhances surveillance capabilities of air traffic control (ATC) as well as improves situational awareness of aircraft pilots through integrated systems such as Traffic Collision Avoidance System (TCAS) and Traffic Information Service-Broadcast (TIS-B). While ADS-B provides highly accurate position data, the occasional instances of intentional or unintentional signal manipulation occur in forms of message jamming, injection and interception [2]. To ensure redundancy and enhance reliability of ADS-B position data, multilateration (MLAT) technique is used as an additional layer of aircraft position verification [3].

In MLAT, the position of the aircraft is determined by analyzing the time difference of arrival (TDOA) of the signal at multiple ground-based receivers. The precision of TDOA measurements, and consequently, the localization accuracy, depends on the synchronization of receiver clocks which presents challenges in practical applications. The Global Positioning System (GPS) can facilitate nanosecond time accuracy, but is not a scalable solution as it requires additional hardware at each receiver [4]. For the receivers in close proximity, a physical link or reference transponder can be used. Although this option is reasonable for surface applications, en-route surveillance requires multiple reference transponders due to line of sight constraints, increasing the complexity and the cost of the system [5].

Additional complication in MLAT arises from the geometric arrangement of the receivers that influence geometric dilution of precision (GDOP). The GDOP value indicates how well-conditioned the set of MLAT equations used to estimate the position is. The lowest GDOP occurs when the transmitter is positioned within the perimeter outlined by receivers that are sufficiently distanced from one another [6]. As the separation between the pair of receivers narrows or the configuration of receivers becomes more linear relative to the transmitter, GDOP related MLAT errors increase [7].

In response to challenges posed by MLAT with TDOA, distance estimation using Received Signal Strength (RSS) has gained attention. RSS is a common feature found in the majority of wireless devices, thus does not require additional hardware and does not have a considerable impact on the local power consumption [8]. The distances between transmitter and receiver required by MLAT equations are usually derived through signal propagation models that relate distance to the attenuation of a signal as it travels through a medium [9]. This relationship is often described with the properties of transmitter and receiver, environmental conditions and signal noise. It has been previously demonstrated, that RSS measurements are inherently susceptible to various environmental factors [10]. Additional complication in RSS-based localization is the variation between theoretical and measurement-based RSS levels depending on the transmitter and receiver properties [11]. This challenge becomes even more prominent when the properties are unknown.

This paper aims to determine the level of aircraft localization accuracy that can be achieved using RSS measurements gathered from low-cost receivers with unknown properties. The data from 43 receivers shown in Fig.1 was acquired from the OpenSky Network [12]. The majority of receivers in this network are RTL-SDR (Software-Defined Radio using Realtek RTL2832U chipset) which is the most common low-cost receiver that allows users to process ADS-B messages. Theoretically, RTL-SDR equipment is capable of achieving time synchronization accuracy sufficient for MLAT with TDOA [13]. However, the location and time synchronization can not be guaranteed for non-verified receivers that comprise about 80% of the network [14]. Moreover, the reference for RSS measurements from each receiver is also unknown.

Fig. 1. Map of OpenSky receiver locations.

Further, this paper elaborates on feasibility of MLAT with RSS by exploring the potential number of aircraft that can be localized using crowdsourced RSS measurements. Additionally, the achievable level of localization accuracy using RSS-based MLAT was investigated. This was accomplished by construction of logarithmic propagation models that describe RSS-distance relationship for each pair of aircraft and receiver present in the OpenSky Network data set. The assessment of model quality was implemented through examination of model-derived distance accuracy and errors in model parameters. This allowed elimination of RSS measurements from faulty transmitters and receivers. Moreover, the sensitivity of localization accuracy to model parameter errors was evaluated for three groups of models with various error cut-off criteria. Finally, the aircraft locations were estimated using MLAT with TDOA and RSS to compare the results in terms of achievable localization accuracy of both methods.

The following content of this paper presents previous work related to the topic in Section II. The methodology of model implementation and subsequent analysis is provided in Section III. The results, summarized in Section IV, are followed by the discussion in Section V. Lastly, the conclusions and recommendations are outlined in Section VI.

II. RELATED WORK

A. Limitations of RSS

The RSS, typically measured in decibel, can vary depending on the characteristics of transmitter and receiver as well as environmental conditions [10]. On the transmitter side, the strength of the signal depends on the hardware employed to generate and amplify the signal. At the receiver, the RSS depends on its sensitivity as well as data processing components. Recommendations for reliable RSS measurements include use of isotropic antennas and measurement calibration [15]. However, ADS-B antennas are often designed with specific radiation patterns to optimize coverage in the desired direction. Moreover, measurement calibration is challenging when the reference for RSS measurements in unknown.

As for the factors related to the environment, RSS measurements are susceptible to signal fading, interference, multipath effect and electromagnetic noise from other devices nearby [10]. It is practically impossible to account for all of these, especially, in networks with multiple receivers. It was previously shown that variations in RSS exist even in ideal, controlled environments [16]. For these reasons, it is considered that using RSS is not an optimal choice for localization purposes [11].

B. Signal propagation models

The attenuation of the signal over the distance is usually described with signal propagation models [9]. In context of aircraft localization, Friis free space model and Log-Distance Path Loss model (LDPL) are widely applied. In Friis free space model, the decrease in received power follows an inverse square decay over the distance. This relationship is given by Eq.1, where P_t and P_r are power transmitted and received, G_t and G_r are gains of transmitter and receiver antennas, d is the distance between them and λ is signal wavelength.

$$\frac{P_r}{P_t} = G_t G_r \left(\frac{\lambda}{4\pi d}\right)^2 \tag{1}$$

A more generalized model that accounts for propagation environment is LDPL given by Eq.2, where PL is path loss, d_0 is close-in reference distance, n is path loss exponent and d is the distance between transmitter and receiver.

$$PL = PL(d_0) + 10nlog_{10}\left(\frac{d}{d_0}\right) \tag{2}$$

The equation above can be extended with the term X_σ to account for random variations in signal power due to disturbances on the propagation path. This is known as Log-normal shadowing model where X_σ is modelled as a zero-mean Gaussian distributed random variable with standard deviation σ. In reality, the noise in ADS-B signal is comprised not only by Gaussian noise, but also by thermal effects as well as outliers caused by undetected garbling [17]. Accounting for these noise sources requires additional monitoring and processing which, in turn, increases complexity of the model.

In general, experiments show a good agreement of ADS-B signal RSS measurements with LDPL model given a complete knowledge of transmitter and receiver properties [18]. In cases when these properties are unknown, previous studies suggest that measurement-based models can be derived. In these models, the unknown terms in equations above can be replaced by parameters that are estimated using the available RSS measurements. The terms in Eq.1 that remain constant during the transmission can be replaced by one parameter resulting in an equation that directly relates RSS to distance [19]. Similarly, the path loss and path loss exponent terms in Eq.2 can be replaced with two individual parameters [20].

Other signal propagation models are available, but not considered in the scope of this paper mainly due to the lack of previous research in context of aircraft localization. Models that were shown to be limited by distance range or transmitter and receiver heights are also not applicable [21].

C. MLAT with RSS

In MLAT with RSS, the distance derived from signal propagation model defines the radius of the circle (in 2D) or the sphere (in 3D) around the receiver. The position of the transmitter is then found at the intersection of these circles or spheres. This localization method offers relative simplicity, thus implementation cost, compared to MLAT with TDOA [22]. However, the application of MLAT with RSS has not been widely explored in outdoor applications mainly due to inherent limitations of RSS discussed in previous sections.

In indoor applications, it has been demonstrated that the localization error of RSS-based MLAT increases as the spatial scale of the considered area expands [23]. This phenomenon is attributed to more pronounced effects of multipath and interference within greater areas. Furthermore, the localization error increases in line with the noise present in the signal [24].

Similar to MLAT with TDOA, the least-squares (LS) algorithm is commonly used for the solution of RSS-based MLAT problems. The primary objective of LS algorithm is to minimize the sum of the squares of the residuals between observed and estimated values. In previous indoor studies, solution of MLAT with RSS using LS algorithm demonstrated a significant increase of localization accuracy compared to the direct solution [24, 25]. However, no research on its implementation in outdoor environments was found.

III. METHODOLOGY

A. Data

The data set used for the analysis was acquired from the OpenSky Network in csv format. This data set contains 4892103 transmissions recorded during one hour and includes the following:

- Transmission ID: identifier of signal transmission by unique aircraft at one instance of time.
- Server timestamp: time of the server in seconds.
- Aircraft number: unique number of the aircraft.
- Aircraft position: WGS84 longitude and latitude in decimal degrees and geometric height in meters.
- Receiver number: unique number of the receiver.
- Receiver position: WGS84 longitude and latitude in decimal degrees and height in meters.
- Timestamp: measured by the receiver in nanoseconds at the time of signal arrival.
- RSS: measured by the receiver in decibel.

Given the WGS84 longitudes (λ) and latitudes (ϕ), the coordinates of aircraft and receivers on Cartesian plane (x, y, z) were found through transformation given by Eqs.3 where R is the radius of the Earth, h is the height above the surface and e^2 is squared eccentricity defined by semi-major and semi-minor axes.

$$\begin{aligned} x &= (R(\phi) + h)\cos(\phi)\cos(\lambda) \\ y &= (R(\phi) + h)\cos(\phi)\sin(\lambda) \\ z &= (R(\phi)(1 - e^2) + h)\sin(\phi) \end{aligned} \tag{3}$$

The Euclidean distances in 3D between aircraft and receivers were then found using Eq.4 where (x_a,y_a,z_a) and

(x_s, y_s, z_s) are positions of aircraft and receiver, respectively. For 2D distances, z terms in Eq.4 were neglected.

$$d = \sqrt{(x_a - x_r)^2 + (y_a - y_r)^2 + (z_a - z_r)^2} \quad (4)$$

B. Logarithmic models

The models relating RSS to distance between aircraft and receiver were constructed on the basis of signal propagation models described in the previous section. The logarithmic model given by Eq.5 was constructed by fusion of Eq.1 and Eq,2 and replacement of unknown terms with parameters. Here, parameter α was introduced to replace the constant terms, such as transmitter and receiver properties independent from distance, while parameter β scales the distance-dependent loss.

$$RSS = \alpha - 10 \cdot \beta \cdot log_{10}(d) \quad (5)$$

With the intention to express the distance in terms of RSS, the resulting model is given by Eq.6 with distance d in meters and RSS in decibel.

$$d = 10^{\left(\frac{\alpha - \text{RSS}}{10\beta}\right)} \quad (6)$$

The model given by Eq.6 was constructed for each aircraft-receiver pair individually. To find parameters α and β that represent the pair, measurements were split into training and testing subsets in proportion 80-20. Aircraft-receiver pairs with more than 100 transmissions were considered to ensure availability of an adequate number of measurements for training and testing of the model. The models were trained using the training subset data only. Later, generalization of each model was evaluated using the testing subset. This was done by calculating the root mean square error (RMSE) given by Eq.7 where $\hat{d_i}$ are the model-predicted distances, d_i are the actual distances and N is the number measurements.

$$RMSE = \sqrt{\frac{1}{N}\sum_{i=1}^{N}(\hat{d_i} - d_i)^2} \quad (7)$$

The consistency between RMSE of training and testing subsets was evaluated in order to assess model performance on previously unseen data. Further, the uncertainties of model parameters α and β were examined by computing relative standard error (RSE) given by Eq.8 where $\sigma_{\bar{\alpha}}$ is the standard deviation of the estimated parameter $\bar{\alpha}$.

$$RSE_{\bar{\alpha}} = \frac{\sigma_{\bar{\alpha}}}{|\bar{\alpha}|} \times 100 \quad (8)$$

Generally, low RSE percentage indicates lower uncertainty of estimated parameters. In previous studies, the cut-off point for RSE classifying parameter estimate as reliable varies between 10% and 20% [26]. Therefore, the sensitivity of localization accuracy to RSE cut-off was examined for values 15%, 10% and 5%.

C. MLAT with TDOA and RSS

In multilateration (MLAT), the hyperbolic curves are used to determine the position of the transmitter. MLAT requires at least three receivers to determine 2D position of the aircraft. With less than three receivers, multiple locations can satisfy the distance measurements resulting in an ambiguous solution [27]. Similarly, four or more receivers are needed to determine 3D position. It should be noted that in 3D MLAT, ground based receivers do not provide sufficient elevation angle diversity needed to resolve the vertical component of GDOP, leading to higher position errors [5].

Due to the line of sight constraint of MLAT, the measurements received from beyond line of sight distance were discarded. These measurements were identified through theoretical line of sight given by Eq.9 where R is the radius of the Earth and h_a and h_r are heights of aircraft and receiver, respectively, in meters.

$$d_{LOS} = \sqrt{2Rh_a + {h_a}^2} + \sqrt{2Rh_r + {h_r}^2} \quad (9)$$

In presence of three receivers (i,j and k) with known coordinates (x_i, y_i, z_i), MLAT equations are given by Eqs.10 where d is the distance to corresponding receiver, t is the timestamp at corresponding receiver and c is signal propagation speed equal to 299792458 m/s.

$$\begin{cases} d_i = \sqrt{(x - x_i)^2 + (y - y_i)^2} \\ d_j = \sqrt{(x - x_j)^2 + (y - y_j)^2} \\ d_k = \sqrt{(x - x_k)^2 + (y - y_k)^2} \\ d_i - d_j = (t_i - t_j)c \\ d_i - d_k = (t_i - t_k)c \\ d_j - d_k = (t_j - t_k)c \end{cases} \quad (10)$$

With n receivers present at the instance of transmission, the number of equations in the resulting MLAT system is given by Eq.11.

$$\frac{n!}{2!(n-2)!} \quad (11)$$

Unlike in MLAT with TDOA, MLAT with RSS does not consider differences between receivers. Therefore, the resulting system is given by the first three equations in Eqs.10. With n receivers, this system contains n equations.

The solutions of MLAT equations were found using LS algorithm. Due to the non-linear nature of the problem, LS requires an initial guess for the location of the transmitter. The midpoint of receivers in view for each transmission instance was computed as the mean of their coordinates and used as an initial guess. The solution accuracy was evaluated with RMSE given by Eq.12 where $(\hat{x}_i,\hat{y}_i)$ is estimated position of the aircraft and (x_i,y_i) is true position.

$$RMSE = \sqrt{\frac{1}{N}\sum_{i=1}^{N}(\hat{x}_i - x_i)^2 + (\hat{y}_i - y_i)^2} \qquad (12)$$

As location and time synchronization of the OpenSky Network receivers can not be verified, the data contains faulty timestamps that result in MLAT with TDOA solution converging to the wrong position. With respect to the presence of faulty solutions, the results were evaluated using RMSE for the range of best solutions found. The results were demonstrated for 100%, 80% and 60% of best solutions.

IV. RESULTS

A. Available data and RSS-distance models

From the initial data set, 0.06% were received from beyond theoretical line of sight distance and were discarded. Additionally, 3806 aircraft-receiver pairs were discarded due to insufficient number of RSS measurements available for model implementation. With the remaining 4888988 transmissions, logarithmic models representing RSS-distance relationships between each aircraft-receiver pair was constructed. An example of the model for receiver 663 with aircraft 2731 is shown in Fig.2.

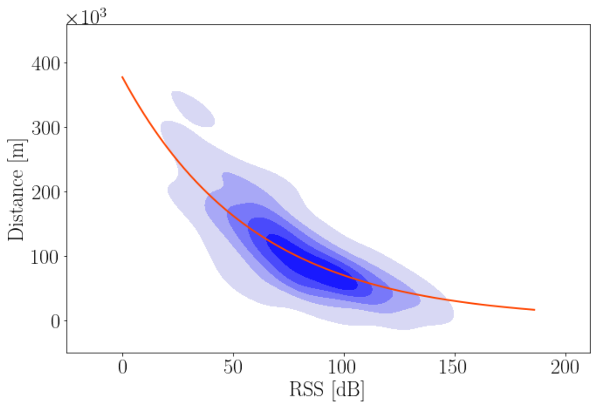

Fig. 2. Distribution of RSS measurements (blue) and logarithmic model (orange) for receiver 663 with aircraft 2731.

From Fig.2, it is clear that most of RSS measurements for this aircraft-receiver pair could be captured by the model quite accurately. This was reflected by the RSE of model parameters which are RSE_α=2.8% and RSE_β=3.6% for the case in Fig.2. However, the model becomes less representative of an actual RSS distribution as the RSE value increases. The examples of RSS distribution with resulting logarithmic model for various RSE cut-off values for one aircraft can be found in Appendix A. It was established that models with RSE values of more than 15% were not representative due to the poor quality of RSS measurement recorded for the specific aircraft-receiver pairs. The numbers of transmissions satisfying the RSE cut-off values along with the number of unique aircraft, receivers and aircraft-receiver pairs are shown in Table I.

Table I. Number of transmissions in models with various RSE cut-off values for 2D and 3D analysis.

	Transmissions	Aircraft	Receivers	Pairs
2D(15%)	1284452	550	39	2763
2D(10%)	875409	401	38	1811
2D(5%)	120276	83	29	277
3D(15%)	493671	314	39	1955
3D(10%)	271870	209	36	1180
3D(5%)	8451	13	20	58

As evident from Table I, at most 550 aircraft could be localized in 2D (314 of which also in 3D) given the RSE cut-off criteria selected. Further, the number of aircraft that are possible to localize decreases with RSE cut-off value as less aircraft-receiver pairs satisfying model parameter error criteria are available. Overall, 26.3% and 10.1% of all transmissions in the initial data set were accounted for in 2D and 3D, respectively, for the highest RSE cut-off value.

B. Model generalization and overall accuracy

The ability of the model to adapt to previously unobserved data or its capacity for generalization was evaluated with RMSE of the training and testing subsets. This assessment was performed across various RSE cut-off values in order to investigate the influence of more refined models on the RMSE of predicted distances.

The distribution of 2D distance RMSE in training and testing subsets for each RSE cut-off group is shown in Fig.3. As evident from the figure, the median RMSE values for both training and testing subsets demonstrate consistency among all RSE cut-off groups. This suggests that the models maintain a stable level of predictive accuracy when confronted with previously unobserved data.

Moreover, the lower RSE cut-off values are indicative of regularity in more accurate distance prediction across all models. This is reflected in the number of outliers present in each group shown in Fig.3. None of the models with RSE cut-off of 5% resulted in significantly higher predicted distance RMSE compared to other models in this group. As the RSE cut-off increases to 10% and 15%, the number of outlier models rises to 27 and 40, respectively.

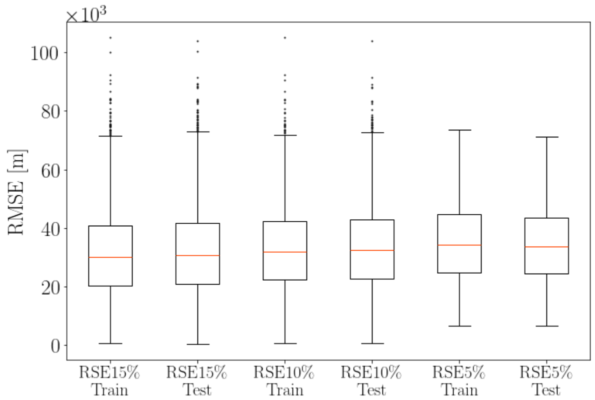

Fig. 3. RMSE distribution in training and testing subsets with RSE cut-off of 15%, 10% and 5% (2D).

The distribution of 3D distance RMSE showed higher regularity of accurate distance prediction resulting in none, 19 and 30 outliers in corresponding RSE cut-off groups.

The overall accuracy of the model-derived distances was evaluated with RMSE for the models within RSE ranges of 0-5%, 5-10% and 10-15%. The RMSE of the model-derived distances in 2D was found at roughly 34, 35.5 and 36 kilometers for models with RSE within the respective range. In 3D, the RMSE of model-derived distances was roughly 35.5, 36.5 and 36.5 kilometers, accordingly.

C. Model-derived distance errors

An accurate estimation of the distance between the aircraft and all receivers in view is necessary for its position estimation. However, the RMSE of model-derived distances found at roughly 35 kilometers in the previous section is not fully representative of model accuracy as the distance between one aircraft and multiple receivers varies. In other words, if the signal is received from the shorter distance, the model prediction results in smaller RMSE regardless of how well the model was able to capture the relationship between RSS and distance. Therefore, RSE is a crucial metric considered along with RMSE to evaluate the uncertainty of model-derived distances.

Hereby, the importance of low RSE of model parameters for accurate position estimation is demonstrated in Fig.4 that shows true and model-derived distances between aircraft 1180 and two receivers: 147 and 632. It is evident that model-derived distances in the top figure are more representative of true distances compared to the bottom figure. This is reflected in lower RSE values of the model: RSE$_\alpha$=1.6% and RSE$_\beta$=1.7% with receiver 147 in contrast with RSE$_\alpha$=7.8% and RSE$_\beta$=8.0% with receiver 632. However, due to the fact that RSS measurements were received from larger distances by receiver 147 compared to receiver 632, the RMSE of model-derived distances in top figure resulted in 22866 meters compared to 7874 meters in bottom figure.

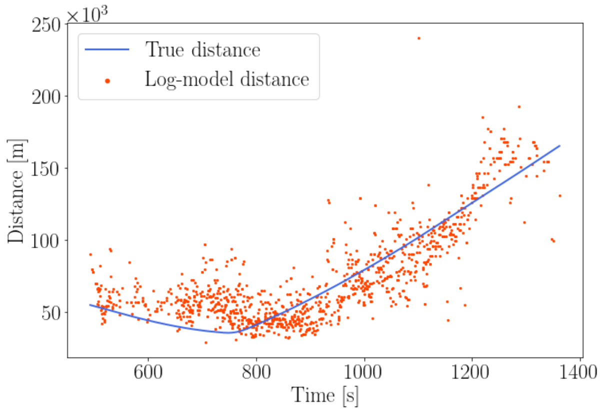

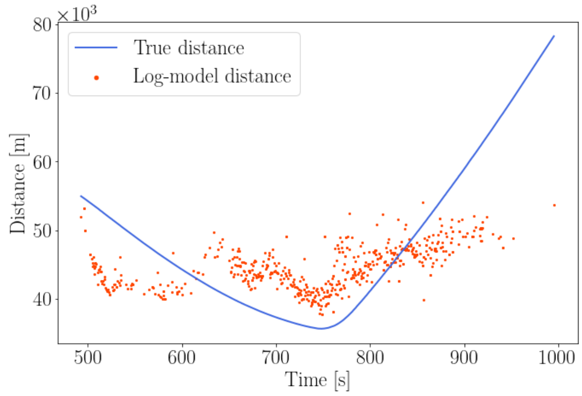

Fig. 4. True and model-derived distances between aircraft 1180 and receiver 147 (top) and receiver 632 (bottom) over the time when RSS measurements were observed.

Further, the importance of RSE in model-derived distance accuracy follows from the definition of RSE that is given by the ratio between standard deviation of the parameter and the parameter itself. Table II summarizes the median of estimated parameters and mean standard deviation of the models with various RSE cut-off values. It is evident that the values of both parameters along with their standard deviation generally increase with the increase of RSE cut-off.

Table II. Median and standard deviation of estimated parameters $\bar{\alpha}$ and $\bar{\beta}$ in subsets with various RSE cut-off values.

RSE	Med($\bar{\alpha}$)	$\sigma_{\bar{\alpha}}$	Med($\bar{\beta}$)	$\sigma_{\bar{\beta}}$
<15%	1445.4	190.2	27.7	3.7
<10%	1249.4	106.5	23.8	2.1
<5%	1061.3	44.7	19.8	0.9

Based on the observed behavior of the curve defined by Eq.6, the model demonstrates pronounced tendency to linearity with the increase of parameters α and β. This can be inspected in the detailed case presented in Appendix B that shows the models and model-derived distances for various RSE cut-off values. The case presented demonstrates the correlation between RSE of model parameters and RMSE of model-derived distances for the models within similar distance range. It is clear that distance errors increase along with the model parameter errors. Furthermore, the ability of the model to capture RSS measurements recorded from larger distances decreases significantly with the increase of parameter RSE due to pronounced tendency to linearity. In other words, the model becomes close to linear as model parameters increase which, in turn, causes the model to neglect the RSS measurements from larger distances.

D. Localization accuracy and RSE of model parameters

Hereby, the results of localization using MLAT with TDOA and MLAT with RSS are discussed with respect to different RSE cut-off groups. To begin with, the RMSE of 2D localization results for each RSE cut-off group are presented in Table III. Due to presence of various not synchronized receivers in the network, all results of MLAT with TDOA are not representative of its general accuracy. Therefore, Table III also demonstrates the RMSE for 80% and 60% of best results obtained using both methods.

Table III. RMSE in meters of 2D localization results using MLAT with TDOA and MLAT with RSS for 60, 80 and 100% of best results in various RSE cut-off groups.

RSE		<5%	<10%	<15%
TDOA	60%	1783.4	1649.6	1594.7
	80%	16707.5	12189.8	11981.6
	100%	2091969.3	1952153.2	1911096.8
RSS	60%	29439.5	30284.4	31839.7
	80%	40222.4	41236.4	43866.1
	100%	68299.1	69613.3	76868.3

It is clear that MLAT with TDOA generally facilitates much higher localization accuracy compared to MLAT with RSS. However, in cases when one or more receiver clocks are not synchronized MLAT with TDOA results in unreasonable errors that are shown as 100% of all results in Table III. Consecutive decrease of accuracy along with RSE cut-off value is attributed to smaller number of receivers available at the moment of each transmission.

Furthermore, MLAT with RSS produced slightly more accurate results when models with lower RSE cut-off values were considered. This trend, evident from Table III, is supported by Fig.5 that shows 2D localization results for aircraft 2834 with RSE cut-offs of 5% in the top figure and 10% in the bottom figure. The differences between these figures were attributed to the receivers number 133 and 257. The RSE values for these aircraft-receiver pairs were found at RSE_α=6.9%, RSE_β=7.4% for receiver 133 and RSE_α=8.0%, RSE_β=8.3% for receiver 257. Therefore, the measurements from these receivers were not considered in MLAT with RSS using models with RSE<5%. As a result, the erroneous cluster of estimated locations in the right side of bottom figure was not evaluated.

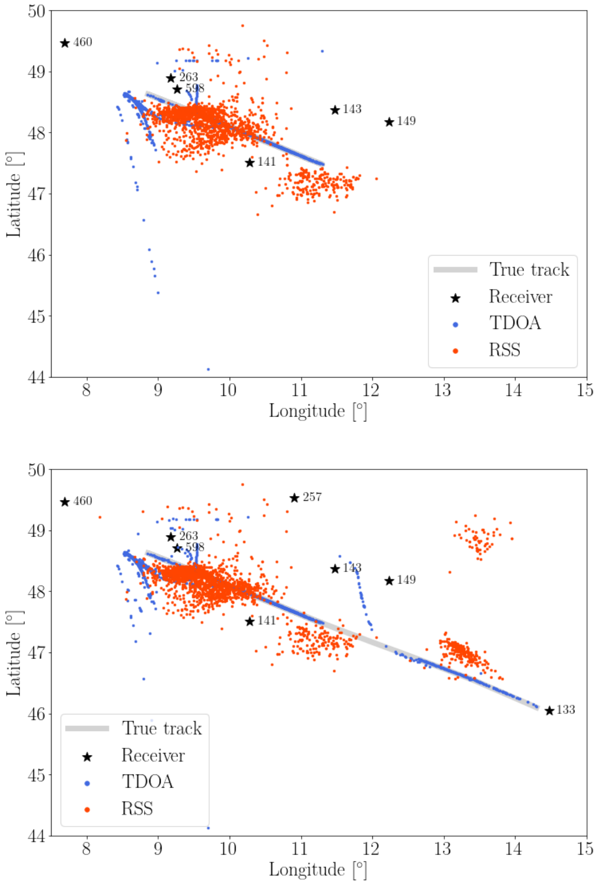

Fig. 5. 2D localization results for aircraft 2834 using MLAT with TDOA (blue) and MLAT with RSS (orange) based on the models with RSE<5% (top) and RSE<10% (bottom).

This in turn leads to lower RMSE of MLAT with RSS which was found at approximately 31.3 kilometers in the top figure in contrast to 33.4 kilometers in the bottom figure for 80% of best solutions. Notably, the timestamp measurements from receivers 133 and 257, along with some of the remaining receivers, were also inaccurate. Therefore, elimination of these receivers resulted in improved MLAT with TDOA accuracy with RMSE values found at 49.1 and 55.0 kilometers accordingly.

E. Localization accuracy in 2D and 3D

The results of 2D localization summarized above demonstrated the trend for improved accuracy of MLAT with RSS using models with smaller RSE cut-off values. A similar trend was observed in 3D localization results. The RMSE values of MLAT with TDOA and MLAT with RSS in 3D for each RSE cut-off group are summarized in Table IV.

Table IV. RMSE in meters of 3D localization results using MLAT with TDOA and MLAT with RSS for 60, 80 and 100% of best results in various RSE cut-off groups.

RSE		<5%	<10%	<15%
TDOA	60%	13475.3	11638.2	9356.8
	80%	21917.1	20426.0	18113.9
	100%	3710335.1	3773518.2	3613642.0
RSS	60%	33825.8	34991.3	35444.1
	80%	40720.7	43604.1	43965.8
	100%	59509.1	62851.1	63040.6

As anticipated, MLAT with TDOA in 3D shows much higher localization errors compared to 2D due to inability to resolve the altitude component. In contrast, MLAT with RSS in 3D demonstrated lower RMSE values for all results considered. The errors of 2D and 3D MLAT with RSS are comparable when 80% of best estimations are considered. However, RMSE increases as more accurate models are evaluated resulting in approximately 29.4 and 33.8 kilometers error in 2D and 3D for the lowest RSE cut-off group.

The comparison of localization results between 2D and 3D is shown on the example of the aircraft number 672 in Fig.6. In this case, comparable RMSE of MLAT with TDOA in 2D (top) and 3D (bottom) was found at 39.7 and 39.9 kilometers accordingly. Notably, MLAT with RSS demonstrated higher accuracy with RMSE of 28.8 kilometers in 2D and 31.1 kilometers in 3D. Such poor performance of MLAT with TDOA is again related to receiver synchronization issues. Along with those, higher errors in 2D MLAT are likely related to geometric arrangement of receivers 147 and 632 that are situated within 50 meters of one another. Such arrangement results in poor geometry that, in turn, affects the accuracy of MLAT. The effect of poor geometry is more pronounced in 2D MLAT where measurements from three receivers are considered. If two out of three receivers are situated in close proximity, high localization errors occur as in the case of the top figure in Fig.6. From the results obtained, it is unclear whether poor geometry has comparable influence on MLAT with RSS.

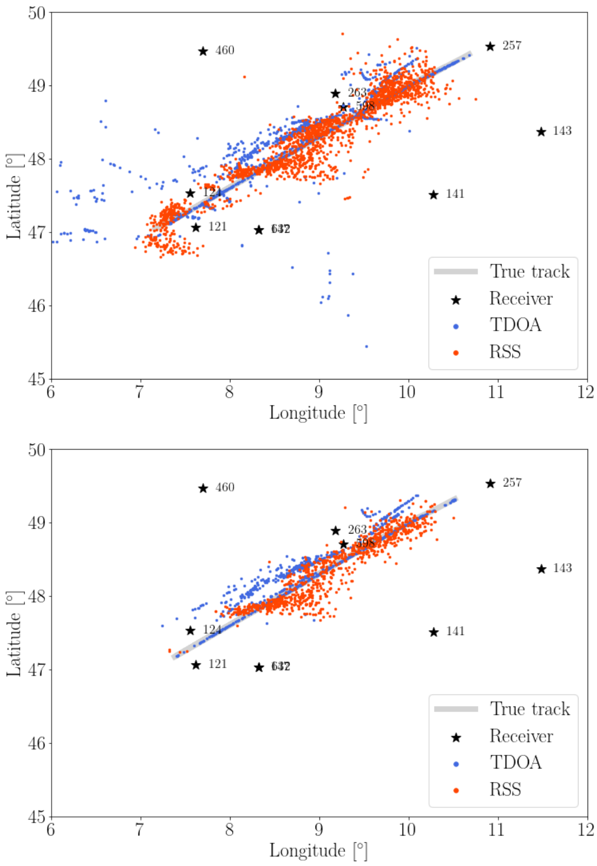

Fig. 6. Localization results for aircraft 672 using MLAT with TDOA (blue) and MLAT with RSS (orange) in 2D (top) and 3D (bottom).

F. Tracking performance

The results demonstrated in Fig.5 and Fig.6 considered two cases when receivers were not synchronized. However, in presence of reliable timestamps, MLAT with TDOA demonstrated significantly higher accuracy compared to MLAT with RSS. This is reflected in localization errors when 80% or less of the best results are considered. In line with precise position estimation, MLAT with TDOA showed much better tracking performance as shown in both cases in Fig.7. Notably, the RSE of model parameters had little to no influence on these results. In the top figure, the average RSE_α and RSE_β among all models were found at 8.8% and 8.9%, respectively, while in the bottom figure these values were 4.8% and 5.1%. Similar to model-derived distances, the localization RMSE in cases shown in Fig.7 should be accounted relative to the distance between aircraft and receivers which is much larger in the top figure. The RMSE of MLAT with RSS for aircraft 2845 (top) and 2804 (bottom) were found at 63.0 and 26.8 kilometers, respectively. Meanwhile, the MLAT with TDOA resulted in RMSE of 1383.4 and 140.1 meters.

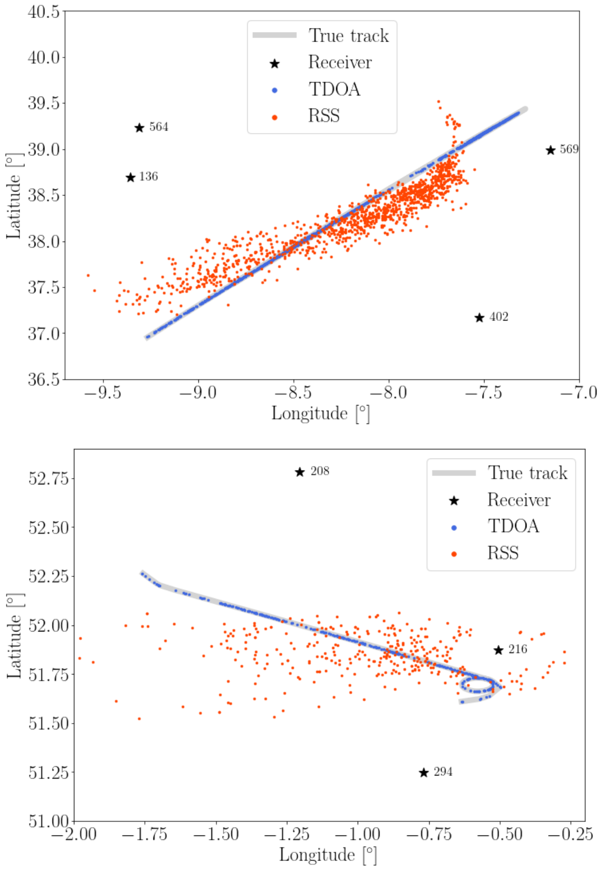

Fig. 7. Tracking performance of MLAT with TDOA (blue) compared to MLAT with RSS (orange) for aircraft 2845 (top) and aircraft 2804 (bottom).

Overall, the most accurate result of MLAT with RSS in 2D and 3D among all RSE cut-off groups was found with RMSE of 9858.6 and 12034.4 meters. For MLAT with TDOA, these values were 118.1 and 205.8 meters.

V. DISCUSSION

A. Feasibility

The feasibility of RSS-based MLAT using crowdsourced measurements attributes to the quality of available RSS measurements and their processing. The results demonstrated that at most 550 aircraft could be localized in 2D using the RSS-distance models with the highest RSE cut-off value of 15%. This quantity accounts for 34.3% of all aircraft registered in the OpenSky Network data set. Meanwhile, the main reason behind poor quality of the models is related to erroneous RSS measurements, some aircraft were not observed long enough by multiple receivers in order to construct the model. Therefore, the number of aircraft possible to localize would be higher provided the data set which is not limited to one hour of observation.

As for the data processing, the solution of MLAT with RSS is less computationally expensive compared to MLAT with TDOA [22]. This is crucial in large receiver networks where the receivers are located in relatively close proximity. With four receivers in view on average during one transmission, the resulting system of equations in MLAT with TDOA contains six equations while MLAT with RSS requires four. As the number of receivers in view and equations in RSS-based MLAT increases to 11 (the maximum number of receivers observed in one transmission), MLAT with TDOA requires 55 equations to be solved. This makes MLAT with RSS computationally more feasible.

The last remark regarding the feasibility of MLAT with RSS attributes its applicability. As the low-cost receivers are widely available and do not require additional hardware or elaborate processing of measurements, MLAT with RSS can provide a reasonable approximation of aircraft position in remote areas without an appropriate infrastructure. This would facilitate not only more extensive coverage, but also availability of data for further research.

B. Logarithmic models

The models of RSS-distance relationship employed in this paper are in logarithmic form. Although it is a common practice to use models of this form to describe signal propagation, other model structures can be applicable given the quality of measurements. It is possible that using polynomial or exponential model would result in more accurate representation of RSS-distance relationship. Furthermore, the variations in RSS measurements can be captured in more detail using non-parametric models. In presence of large quantity of faulty RSS measurements, it is unclear whether capturing these in more detail can possibly result in more accurate localization.

C. Error metrics

The accuracy of RSS-based MLAT is mainly dependent on the quality of propagation models constructed. The approach selected for model quality evaluation was an examination of RSE in the resulting model parameters. It was demonstrated that RSE cut-off value of 20% recommended by previous studies [26] is too large for quality evaluation of the model specific to this research. Various models with RSE values larger than 10% were not representative of the actual RSS measurement distribution mainly due to the poor quality of measurements themselves. Although RSE was shown to be effective in evaluation of how well the models fit the available RSS measurements, it became less useful in presence of faulty transmitters or receivers resulting in highly linear models. Consequently, the correlation between larger RSE of model parameters and model linearity was established.

The second error metric used in the analysis was RMSE of model-predicted distances and model-estimated positions. As in the last case presented, the localization error of MLAT with RSS increased along with the spatial scale of the area considered. Therefore, the RMSE values are higher in situations when the aircraft are at greater distances from receivers. This observation is in line with the previous studies [23]. To be more representative in comparison between different cases, RMSE values can be normalized by mean, standard deviation or interquartile range of the measurements. However, an absolute scale of localization errors considered in this paper would be obscured by normalization.

D. Overall localization accuracy

The poor localization accuracy of MLAT with RSS compared to MLAT with TDOA has already been suggested by the previous research [11]. The results obtained in this paper confirmed that RSS-based MLAT is significantly less accurate compared to the time-based method. Nevertheless, MLAT with RSS demonstrated a comparable localization accuracy level in 2D and 3D which was not the case in MLAT with TDOA that is significantly less precise in 3D. This is attributed to more complex geometric properties of hyperboloids in 3D as well as number of receivers in view. While the availability of smaller number of receivers in groups with lower model parameter errors clearly reduced the accuracy of MLAT with TDOA, MLAT with RSS demonstrated an accuracy improvement by about two kilometers between highest and lowest error groups. The hyperbolic nature of MLAT with TDOA is generally more sensitive to small number of receivers compared to quadratic MLAT with RSS. However, both are influenced by the geometric arrangement of receivers. From the results obtained, the extent of receiver geometry contribution in MLAT with RSS is unclear.

Lastly, the tracking performance of both localization methods was compared indicating a significantly better performance of MLAT with TDOA. Given the reliable receiver timestamp measurements, the track of the aircraft was reconstructed with the accuracy up to 118.1 meters. Not only the overall accuracy of MLAT with RSS was worse, but also the tracking ability. While the reasonable estimation of aircraft position could be obtained, it was practically impossible to reconstruct the track of the aircraft given the dispersed nature of solutions.

VI. CONCLUSION AND RECOMMENDATIONS

The aim of this paper was to investigate the level of localization accuracy that can be achieved using crowdsourced RSS measurements. These were used to construct parameterized propagation models that capture RSS-distance relationship of each individual pair of aircraft and receiver in the OpenSky Network data. Results demonstrated that only a fraction of measurements could be accurately represented by this model facilitating the analysis of 26.3% of all transmissions. This rather low quantity was attributed to the poor quality of available measurements that emerges in high model parameter errors with faulty transmitters or receivers.

Further, this paper set a baseline for the research in RSS-based MLAT by demonstrating the method for model application for localization purposes. The results showed comparable or improved accuracy of MLAT with RSS to MLAT with TDOA in cases when receivers were not synchronized. However, the general performance of MLAT with RSS was significantly less accurate in presence of reliable receiver timestamps for time-based MLAT. The evaluation of RSS-based MLAT error sensitivity to model parameter errors showed a minor reduction in localization error when more accurate models were considered. This suggests that the localization accuracy can be further improved by using RSS measurements from reliable transmitter-receiver pairs only or by measurement calibration. The most accurate results obtained in this paper were found with RMSE of 118.1 and 9858.6 meters in 2D MLAT with TDOA and RSS, respectively.

The recommendations for further research are related to the method of model implementation and quality of available data. For the models with low parameter errors, further investigation into random RSS variations or noise in RSS measurements can be implemented. It is possible, that better representation of RSS-distance relationship can be obtained by filtering, smoothing or complete removal of outliers in the available RSS measurements. Additionally, the influence of receiver geometry on the accuracy of MLAT with RSS can be examined to compare the localization accuracy degradation to that observed in MLAT with TDOA. Lastly, the methodology of this research can be applied on data from receivers with known properties, reference for RSS measurements and verified locations to investigate the achievable level of localization accuracy in scenario with less uncertainties.

REFERENCES

[1] Rekkas, C., "Status of WAM, ADS-B out and ATSAW deployment in Europe," *2014 Tyrrhenian International Workshop on Digital Communications - Enhanced Surveillance of Aircraft and Vehicles (TIWDC/ESAV)*, 2014, pp. 1–5.

[2] McCallie, D., Butts, J., and Mills, R., "Security analysis of the ADS-B implementation in the next generation air transportation system," *International Journal of Critical Infrastructure Protection*, Vol. 4, No. 2, 2011, pp. 78–87.

[3] Chen, Y., and Zhou, L., "Vulnerabilities in ADS-B and Verification Method," *2020 IEEE 2nd International Confer-*

ence on Civil Aviation Safety and Information Technology (ICCASIT), 2020, pp. 90–94.

[4] Chefrour, D., "Evolution of network time synchronization towards nanoseconds accuracy: A survey," *Computer Communications*, Vol. 191, 2022, pp. 26–35.

[5] Galati, G., Leonardi, M., Magaro, P., and Paciucci, V., "Wide area surveillance using SSR mode S multilateration: advantages and limitations," *European Radar Conference, 2005. EURAD 2005.*, 2005, pp. 225–229.

[6] Zhao, Y., Lung, C.-H., Lambadaris, I., and Goel, N., "Improving Location Identification in Wireless Ad Hoc/Sensor Networks Using GDOP Theory," *2009 Third International Conference on Sensor Technologies and Applications*, 2009, pp. 223–228.

[7] Bronk, K., and Stefanski, J., "Bad Geometry Influence on Positioning Accuracy in Wireless Networks," *EUROCON 2007 - The International Conference on "Computer as a Tool"*, 2007, pp. 1131–1135.

[8] Mao, G., Fidan, B., and Anderson, B., "Wireless sensor network localization techniques," *Computer Networks*, Vol. 51, No. 10, 2007, pp. 2529–2553.

[9] Rappaport, T., *"Wireless Communications: Principles and Practice"*, 2nd ed., Prentice Hall PTR, 2002.

[10] Capriglione, D., Ferrigno, L., D'Orazio, E., Paciello, V., and Pietrosanto, A., "Reliability analysis of RSSI for localization in small scale WSNs," *2012 IEEE International Instrumentation and Measurement Technology Conference Proceedings*, 2012, pp. 935–940.

[11] Heurtefeux, K., and Valois, F., "Is RSSI a Good Choice for Localization in Wireless Sensor Network?" *2012 IEEE 26th International Conference on Advanced Information Networking and Applications*, 2012, pp. 732–739.

[12] Schäfer, M., Strohmeier, M., Lenders, V., Martinovic, I., and Wilhelm, M., "Bringing up OpenSky: A large-scale ADS-B sensor network for research," *IPSN-14 Proceedings of the 13th International Symposium on Information Processing in Sensor Networks*, 2014, pp. 83–94.

[13] Li, A., and Zheng, Y., "Research and Implementation of Wireless TDOA Positioning Station Synchronization Based on RTL-SDR," *2022 IEEE 6th Information Technology and Mechatronics Engineering Conference (ITOEC)*, Vol. 6, 2022, pp. 1087–1090.

[14] Schäfer, M., Strohmeier, M., Leonardi, M., and Lenders, V., "LocaRDS: A Localization Reference Data Set," *Sensors*, Vol. 21, No. 16, 2021, p. 5516.

[15] Zanella, A., "Best Practice in RSS Measurements and Ranging," *IEEE Communications Surveys & Tutorials*, Vol. 18, No. 4, 2016, pp. 2662–2686.

[16] Azmi, K. H. M., Berber, S. M., and Neve, M. J., "The influence of received signal strength measurement methods on the accuracy of distance estimation in wireless sensor network," *2017 IEEE 4th International Conference on Smart Instrumentation, Measurement and Application (ICSIMA)*, 2017, pp. 1–5.

[17] Pawlitzki, A., and Neufeldt, H., "Real time performance monitoring and noise analysis in an operational WAM system," *2011 Tyrrhenian International Workshop on Digital Communications - Enhanced Surveillance of Aircraft and Vehicles*, 2011, pp. 207–212.

[18] Naganawa, J., Honda, J., Otsuyama, T., Tajima, H., and Miyazaki, H., "Evaluating Path Loss by Extended Squitter Signals for Aeronautical Surveillance," *IEEE Antennas and Wireless Propagation Letters*, Vol. 16, 2017, pp. 1353–1356.

[19] Sun, J., and Hoekstra, J., "Analyzing Aircraft Surveillance Signal Quality at the 1090 Megahertz Radio Frequency," 2020.

[20] Schäfer, M., Strohmeier, M., Lenders, V., Martinovic, I., and Wilhelm, M., "Bringing up OpenSky: A large-scale ADS-B sensor network for research," *IPSN-14 Proceedings of the 13th International Symposium on Information Processing in Sensor Networks*, 2014, pp. 83–94.

[21] Mahmood, T., AL-Qaysi, H. K., and Hameed, A. S., "The Effect of Antenna Height on the Performance of the Okumura/Hata Model Under Different Environments Propagation," *2021 International Conference on Intelligent Technologies (CONIT)*, 2021, pp. 1–4.

[22] Bohidar, S., Behera, S., and Tripathy, C. R., "A comparative view on received signal strength (RSS) based location estimation in WSN," *2015 IEEE International Conference on Engineering and Technology (ICETECH)*, 2015, pp. 1–7.

[23] Barodi, L., and Dağ, T., "The Performance of the RSS-Based Lateration Algorithm for Indoor Localization," *2019 International Conference on Sustainable Information Engineering and Technology (SIET)*, 2019, pp. 148–153.

[24] Cengiz, K., "Comprehensive Analysis on Least-Squares Lateration for Indoor Positioning Systems," *IEEE Internet of Things Journal*, Vol. 8, No. 4, 2021, pp. 2842–2856.

[25] Dag, T., and Arsan, T., "Received signal strength based least squares lateration algorithm for indoor localization," *Computers & Electrical Engineering*, Vol. 66, 2018, pp. 114–126.

[26] Sileshi, G., "The relative standard error as an easy index for checking the reliability of regression coefficients," 2015. doi: 10.13140/RG.2.1.2123.6968.

[27] Xinxin, P., Zhigang, H., Jun, Z., Yanbo, Z., and Wei, L., "An approach for close-form solution of multilateration equations," *2010 8th World Congress on Intelligent Control and Automation*, 2010, pp. 5464–5468.

APPENDIX

A. Distribution of RSS measurements (blue) and logarithmic models (orange) for aircraft 2731 with receivers 663, 460 and 10.

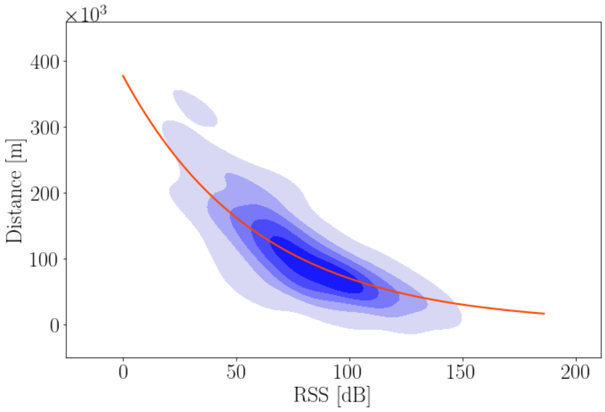

(a) Receiver 663:
RSE$_\alpha$=2.9%, RSE$_\beta$=3.1%

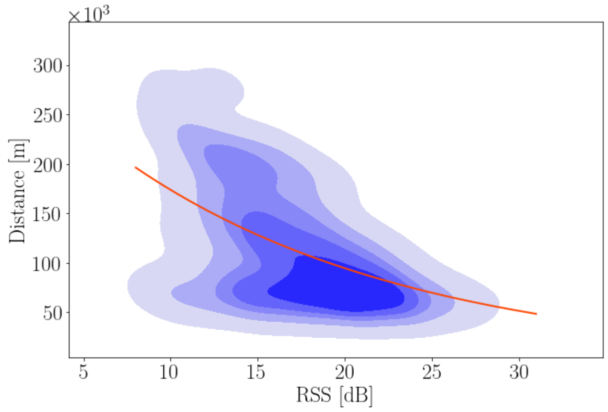

(b) Receiver 460:
RSE$_\alpha$=5.0%, RSE$_\beta$=5.4%

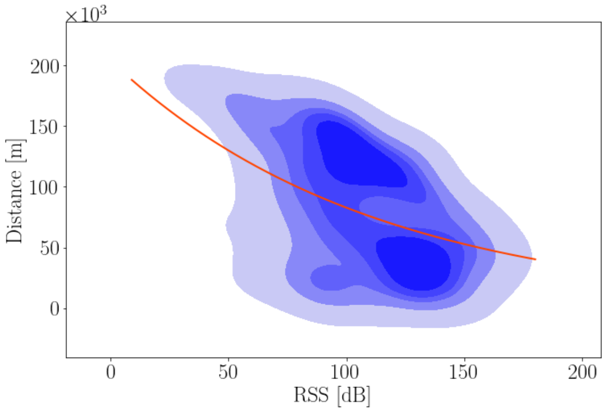

(c) Receiver 632:
RSE$_\alpha$=10.3%, RSE$_\beta$=10.6%

B. RSS-distance models (left) and model-derived distances (right) for aircraft 163 with receivers 147, 598 and 663.

(a) Receiver 147: RMSE = 35815 m, α = 777.4, β= 13.9, RSE$_{\alpha}$=1.9%, RSE$_{\beta}$=2.0%.

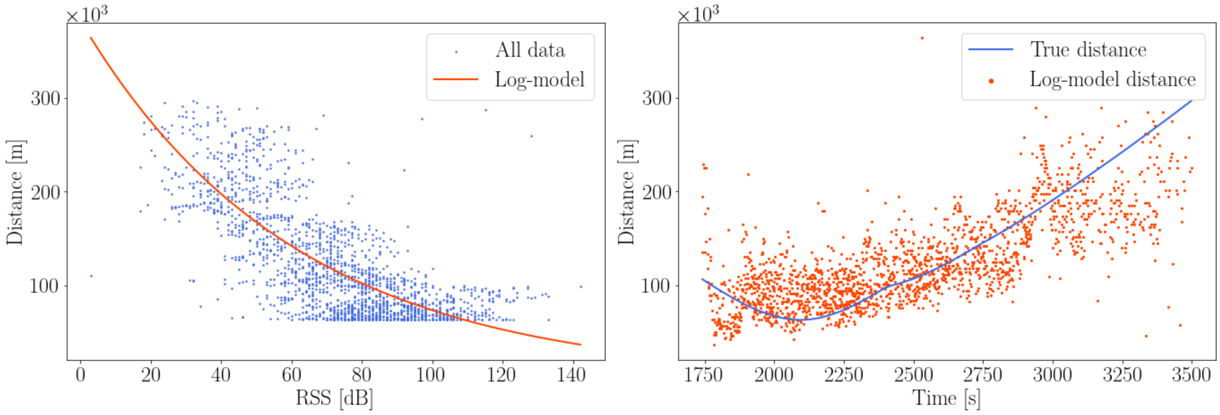

(b) Receiver 598: RMSE = 37666 m, α = 979.5, β= 18.0, RSE$_{\alpha}$=5.0%, RSE$_{\beta}$=5.2%.

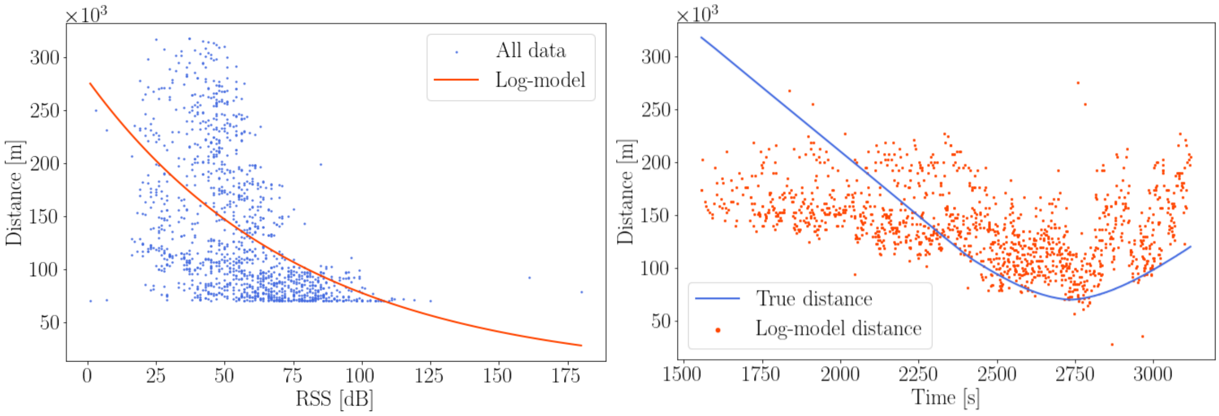

(c) Receiver 663: RMSE = 41545 m, α = 1815.6, β= 34.0, RSE$_{\alpha}$=10.4%, RSE$_{\beta}$=10.6%.

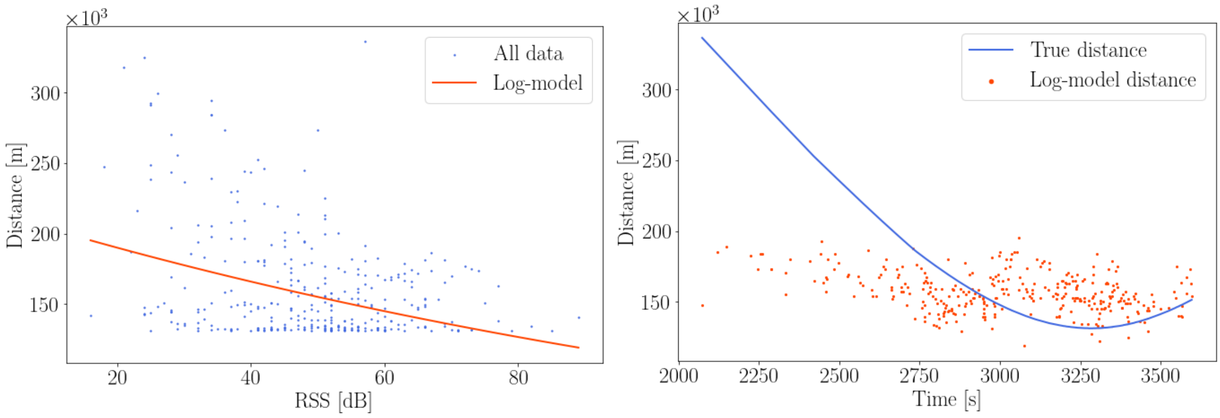

This page intentionally left blank.

II

Preliminary report

Previously graded under AE4020

This page intentionally left blank.

1

Introduction

In the recent years, a significant shift in air traffic surveillance methods occurred, with Automatic Dependent Surveillance-Broadcast (ADS-B) emerging as a promising alternative to traditional radar systems. ADS-B employs the onboard transponder to broadcast the real-time information without a need for the interrogation from the ground. The advantages of such system include an improved precision in tracking, broader coverage through satellite network and reduced operational and maintenance cost. As the momentum behind adopting ADS-B as a primary surveillance tool increases, it highlights the need to explore and enhance its localization capabilities.

The system that has fully integrated the use of ADS-B is the Advanced Surface Movement Guidance and Control System (A-SMGCS) that provides services for approach and ground surveillance in airports with high level of accuracy [1]. The A-SMGCS utilizes the multilateration (MLAT) technique that allows aircraft localization by measuring Time Difference of Arrival (TDOA) of signals received by multiple ground-based receivers. The precision of A-SMGCS is ensured by the strategic placement of ground receivers around the surface of the airport and time synchronization assurance. This highlights the main disadvantages of MLAT when employed in a less regulated setting such as en-route surveillance. Among these, the time synchronization between the receivers is a major issue for TDOA-based localization. Although the GPS allows synchronization with high accuracy, it requires additional equipment or use of the advanced synchronization protocols [2]. It is also not available during the GPS outages. Another issue arises from the geometric arrangements of the receivers [3]. To facilitate an accurate TDOA-based localization, the receivers have to be sufficiently distanced from one another and enclose the transmitter with their perimeter.

The exploration of integrating the received signal strength (RSS) measurements from ADS-B signals has gained attention in response to challenges posed by MLAT limitations. The RSS provides a valuable insight into the signal propagation characteristics, allowing for localization in non-line-of-sight conditions and the mitigation of receiver geometry-related challenges. Moreover, RSS does not depend on time alleviating the synchronization concerns. Yet the RSS measurements are inherently susceptible to environmental factors, including fading, interference and multipath effect. For this reason, it is considered that RSS alone is a bad choice for localization purposes [4]. However, the state-of-art studies suggest that given a good quality of RSS data and the knowledge of propagation parameters, the RSS-based localization accuracy can be significantly improved.

Due to the reduction of RSS with distance, the networks for RSS-based localization have to contain a large number of receivers to allow a good coverage of a wide area. An example of such network is LocaRDS, an open reference data set that contains ADS-B data recorded from crowdsourced receivers by the OpenSky Network [5]. The distribution of LocaRDS receivers and the recorded data are shown in 1.1. Although such networks provide coverage in areas where traditional surveillance systems might have a limited reach, the diversity of receiver characteristics and the potential for biased data collection must be carefully managed to maintain the reliability.

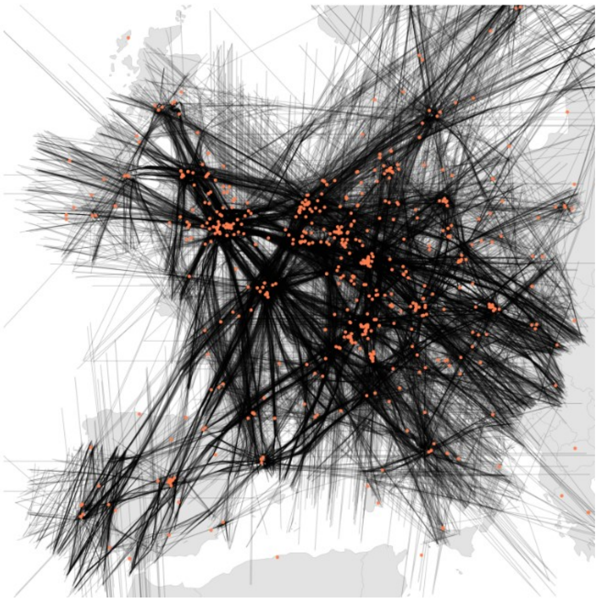

Figure 1.1: LocaRDS receivers (orange) and aircraft positions (black). Adapted from [5].

The main objective of this thesis is to determine whether the use of crowdsourced RSS data is feasible in localization context. In addition, the research aims to compare the difference in localization errors between traditional MLAT technique and RSS-based methods. The central question of this thesis is therefore:

How can crowdsourced measurements of received signal strength improve the accuracy of aircraft localization?

To answer this question, this thesis will focus on the reliability of the crowdsourced data, applicability of signal propagation models and localization accuracy of TDOA- and RSS-based methods. In this report, the exploratory phase results of the thesis are presented and include the establishment of the data set that can be used for further investigation.

The following content of this report is divided in four chapters. Chapter 2 presents the literature review on topics related to enhancing aircraft MLAT using RSS. In chapter 3, the research proposal is drawn along with methodology and planning. In chapter 4, the preliminary results are presented. Lastly, this report is concluded in chapter 5.

2
Literature review

The literature review aims to provide a comprehensive overview of prior studies on topics related to enhancing aircraft multilateration using received signal strength. First, the theory relevant to signal propagation is summarized in section 2.1. With the knowledge of the theory, signal propagation models applicable for aircraft localization purposes are presented in section 2.2. Section 2.3 deals with the specifics of ADS-B signals and their potential limitations. After, localization methods and algorithms that can be applied to ADS-B signals are discussed in sections 2.4 and 2.5 respectively. The last section 2.6 outlines the most crucial findings of this literature review.

2.1. Signal propagation theory

The simplest form of radio wave propagation is known as free-space propagation. It is a particular case of line-of-sight (LOS) propagation, when signal takes a direct path to travel between the transmitter and receiver, unobstructed by obstacles. The theoretical LOS distance that depends solely on the heights of the transmitter h_t and receiver h_r is given by equation 2.1.

$$d_{LOS} = \sqrt{2 * h_t * R + {h_t}^2} + \sqrt{2 * h_r * R + {h_r}^2} \tag{2.1}$$

However, in presence of buildings, vegetation and ground proximity, signal propagation consists of reflection, diffraction and scattering that lead to signal fading that occurs on a small- or a large-scale. In addition, received signals are always susceptible to unwanted fluctuations and disturbances known as noise. These processes are briefly discussed in this section.

2.1.1. Small-scale fading

Small-scale fading, also known as fast fading, refers to rapid variations in amplitude and phase of the signal over a short period of time or distance. It is caused by interference of two or more signal versions that travel different paths to the receiver. For static objects, small-scale fading is an entirely spatial phenomenon called multipath effect, whereas for moving objects, each of the multiple paths experiences an apparent shift in frequency.

Multipath effect is more pronounced in the environments with reflective surfaces, such as urban areas and indoors, but should also be considered when the receiver is elevated above the ground level as shown in figure 2.1(a). Propagation in multiple paths results in frequency modulation due to Doppler shifts, time dispersion caused by propagation delays and rapid changes of signal strength [6]. Although the attenuation of the signal can be constructive and destructive in terms of received signal strength, the latter is dominant in presence of multipath. Therefore, signal detection probability decreases in presence of multipath effect [7].

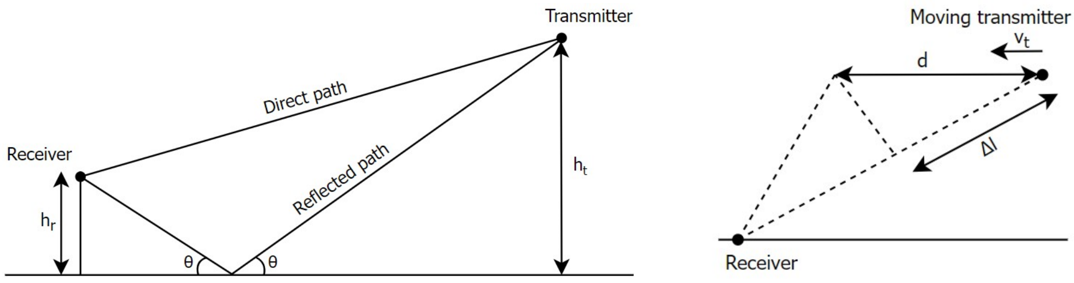

(a) Multipath geometry

(b) Doppler shift geometry

Figure 2.1: Small-scale fading mechanisms.

Doppler shift is an apparent change in signal frequency that occurs when the transmitter is in motion relative to the receiver as shown in figure 2.1(b). The frequency of received signal increases or decreases compared to the transmitted frequency depending on the direction and speed of movement which, in turn, causes variations in the power of the received signal within a certain bandwidth. Monitoring these frequency shifts allows to obtain the trajectory of moving vehicles such as aircraft [8], but significantly lacks accuracy in determining its exact position. However, positioning accuracy can be improved given the additional knowledge of Doppler rate and time delay [9].

2.1.2. Large-scale fading

Large-scale fading, also known as slow fading or shadowing, is the reduction of signal strength with the increase of distance between the transmitter and receiver. Higher frequency signals are more susceptible to large-scale fading due to their shorter wavelengths. In practice, signal attenuation can be mathematically described by path loss models that account for distance along with other parameters relevant in context of signal propagation (see chapter 2.2).

2.1.3. Noise

In addition to fading, signal propagation is susceptible to unwanted fluctuations and disturbances knows as signal noise. The noise present in the signal is quantified by Signal-to-Noise Ratio (SNR) which is the ratio between power of signal and power of noise. When the exact power measurements are not available, SNR is the ratio between mean and standard deviation of received signal strength. In context of localization, knowledge of SNR can alleviate the effect of noise specifically in case when the received signal strength is low [10]. In signal propagation models, such as log-normal shadowing, noise is often assumed to be Gaussian - a statistical noise with normal distribution. However, it was shown that, in reality, the noise in ADS-B received signals is not purely Gaussian, but is comprised of the Gaussian noise, flicker noise caused by thermal and propagation effects as well as outliers caused by undetected garbling of signals [11].

Moreover, weather conditions can also introduce the additional sources of noise and interference to the signal. Due to the dynamic nature, unsteady weather conditions take part in signal degradation especially in presence of wind gusts and precipitation [12]. Although demonstrating minor contribution, the effects of precipitation are not only excluded from common signal propagation models, but were also shown to be underestimated in the conventional rain attenuation model. Lastly, SNR notably decreases along with received signal strength during snowfall [13].

2.2. Signal propagation models

The reduction of signal strength as it propagates through a medium over the distance is known as path loss (PL), thus the models that relate signal strength to distance are referred to as path loss models. In this section, models applicable to aircraft localization are discussed.

2.2.1. Log-distance path loss model

Log-distance path loss model (LDPL) suggests an inverse logarithmic or power law relationship between signal strength and distance [6]. The path loss in decibel is described by equation 2.2 where n is the path loss exponent, d_0 is the close-in reference distance determined from measurements and d is the distance between transmitter and receiver.

$$PL(d) = PL(d_0) + 10n\log_{10}\left(\frac{d}{d_0}\right) \tag{2.2}$$

The path loss exponent n expresses the rate at which the PL increases with distance and depends on the propagation environment (see table 2.1). A measurement based model for the received signal strength can be derived from LDPL in equation 2.2 [14]. In this model, the constants such as transmitter power P_t and antenna gains C are combined into received signal strength at close-in distance $RSS(d_0)$ as shown in eqtheseuation 2.3.

$$RSS(d) = P_t - PL(d) - C = RSS(d_0) - 10n\log_{10}\left(\frac{d}{d_0}\right) \tag{2.3}$$

Table 2.1: Path loss exponent n for different environments. Adapted from [6].

Environment	**Path loss exponent n**
Free space	2
Urban area cellular radio	2.7 to 3.5
Shadowed urban cellular radio	3 to 5
In building line-of-sight	1.6 to 1.8
Obstructed in buildings	4 to 6
Obstructed in factories	2 to 3

Experiments show a good agreement of ADS-B signal measurements with the path loss model given a complete knowledge of transmitter and receiver properties [15]. Although the airframe blockage of the signal is observed during the maneuvers, the measurements observed right after them comply well with the model.

2.2.2. Log-normal shadowing

Log-normal shadowing model is an expansion of LDPL model that accounts for random variations in signal power at equal distance from observer due to disturbances on the propagation path. The shadowing model is given by equation 2.4 where X_σ is a zero-mean Gaussian distributed random variable in decibel with standard deviation σ.

$$PL(d) = PL(d_0) + 10n\log_{10}\left(\frac{d}{d_0}\right) + X_\sigma \quad (2.4)$$

2.2.3. Friis free space model

In situations where the transmitter and receiver have unobstructed line-of-sight (LOS) path between them, Friis free space model predicts that the decrease in received power or signal strength obeys the power law, namely, inverse square decay [6]. The relation of received power P_r to transmitted power P_t in Watt is defined by equation 2.5 where G_r and G_t are the gains of transmitter and receiver antennas, λ is the wavelength in meters and d is the distance between transmitter and receiver, also in meters.

$$\frac{P_r}{P_t} = G_t G_r \left(\frac{\lambda}{4\pi d}\right)^2 \quad (2.5)$$

Similarly to LDPL, the measurement based model for the RSS can be derived from Friis free space model. The terms in equation 2.5 that remain constant during the transmission (antenna parameters, wavelength and relatively constant transmission power) can be replaced by parameter k [16]. Expressed in decibel, the signal strength at the receiver L_r is given by equation 2.6.

$$L_r = k - 20\log_{10} d \quad (2.6)$$

2.2.4. Two ray ground reflection model

Two ray ground reflection model given by equation 2.7 is an extension of Friis free space model that accounts for multipath effect by integrating heights of transmitter h_t and receiver h_r. The model is more suitable in presence of a strong ground reflection component such as smooth reflective surfaces and small angles of transmission.

$$\frac{P_r}{P_t} = G_t G_r \frac{{h_t}^2 {h_r}^2}{d^4} \quad (2.7)$$

It should be noted that at distances d >> $\sqrt{h_t h_r}$, the received signal power decreases with distance more rapidly than in the free space model. This critical distance is given by equation 2.8.

$$d_{critical} = 4\frac{h_t h_r}{\lambda} \quad (2.8)$$

2.2.5. Hata-Okumura model

Hata-Okumura model for path loss estimation was developed for application in urban and suburban environments. The model is given by equation 2.9 where path loss depends on frequency f, receiver antenna height h_t and terrain characteristics factor C.

$$PL(d) = 69.55 + 26.16\log(f) - 13.82\log(h_t) - C + (44.9 - 6.55\log(h_t)) - 5.4 \quad (2.9)$$

Although the model is widely applied as a planning tool for wireless systems, it might not be applicable for aircraft localization as it is only accurate within certain ranges. The application ranges of Hata-Okumura model include frequency range of 150MHz-1.92GHz, distance range of 1-100km and transmitting antenna heights of 30-100m [17].

2.3. Automatic Dependent Surveillance - Broadcast

Automatic Dependent Surveillance–Broadcast (ADS–B) is a surveillance technology that combines GPS positioning, avionics and ground infrastructure to facilitate accurate aircraft surveillance. In other words, an aircraft determines its position and velocity and periodically broadcasts this information with no surveillance interrogation required. In addition to its role in airport and en-route Air Traffic Control, ADS-B is an integrated part of onboard systems such as Traffic Collision Avoidance System (TCAS) and Traffic Information Services - Broadcast (TIS-B). Full system architecture of ADS-B is shown in figure 2.2.

ADS-B messages are transmitted through 1090ES standard data link, that is a Mode S Extended Squitter transponder that operates on 1090 MHz frequency. This channel is also utilized for interrogations and responses of Mode S and related Mode A and C systems (ground surveillance radars) that account for the majority of 1090ES traffic. In high-density airspaces, ADS-B message quality degradation and loss are caused by collision in random access channel [18].

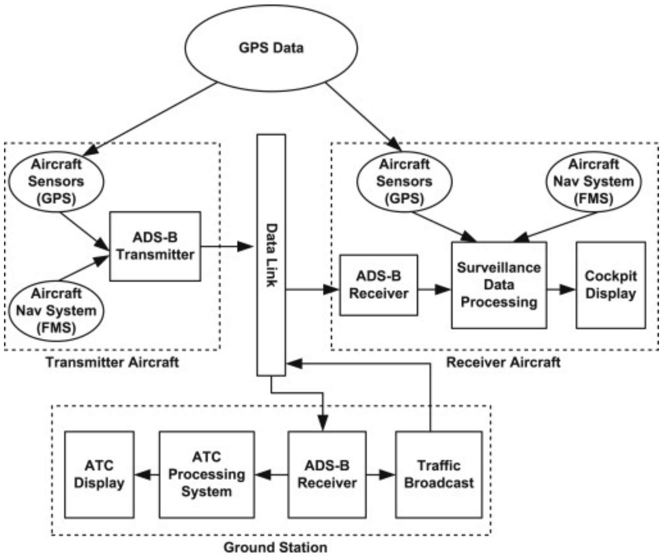

Figure 2.2: ADS-B system components. Adapted from [19].

2.3.1. ADS-B message

ADS-B frame is 112 bits long as shown in figure 2.3. First, 5 bit long downlink format indicates the type of message and is set to 17 (or 10001 in binary) for ES messages. Later, 3 bits indicate Mode S transponder capability. This is followed by a 24 bit long unique transponder code or ICAO aircraft address. Then, the actual ADS-B data or message takes 56 bits and includes identification, position, velocity, urgency code and quality level. Last 24 bits of parity are used by receivers for transmission error detection.

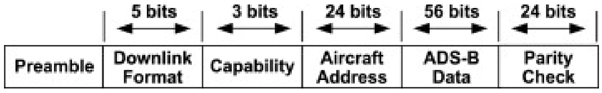

Figure 2.3: ADS-B 1090ES message format. Adapted from [19].

ADS-B messages are not encrypted, thus can be received and interpreted by anyone in possession of appropriate receiving equipment. This results in the potential for malicious exploitation, such as message interception, injection and jamming, that pose significant security issues which are actively addressed by present day research [19]. On the other hand, open access to ADS-B messages allows the development and improvement of aircraft localization methods.

2.3.2. Research data content and limitations

The data employed in this thesis is LocaRDS, an open reference data set that contains ADS-B data recorded from crowdsourced receivers by the OpenSky Network [5]. For localization purposes, the Euclidean distances between transmitters and receivers can be derived from WGS84 longitudes (λ), latitudes (ϕ) and heights (h) in LocaRDS through transformation to Cartesian coordinates given by equations 2.10.

$$\begin{aligned} x &= (R(\phi) + h)cos(\phi)cos(\lambda) \\ y &= (R(\phi) + h)cos(\phi)sin(\lambda) \\ z &= (R(\phi)(1 - e^2) + h)sin(\phi) \end{aligned} \tag{2.10}$$

In this transformation, the radius of curvature in prime vertical $R(\phi)$ is given by equation 2.11 with semi-major and semi-minor axes of WGS84 ellipsoid a = 6378137 m and b = 6356752.314245 m, respectively.

$$\begin{aligned} R(\phi) &= \frac{a}{\sqrt{1 - e^2 sin^2(\phi)}} \\ e^2 &= 1 - \frac{b^2}{a^2} \end{aligned} \tag{2.11}$$

With transformed coordinates of the aircraft with subscript a and receiver with subscript r, the Euclidean distance between them is given by equation 2.12.

$$d = \sqrt{(x_a - x_r)^2 + (y_a - y_r)^2 + (z_a - z_r)^2} \tag{2.12}$$

Besides WGS84 coordinates of transmitters and receivers, LocaRDS provides receiver and server timestamps and received signal strength measurements. Full description of data can be found in Appendix A. The limited accuracy of this data is attributed to the equipment and data processing utilized by contributors of OpenSky Network.

RTL-SDR (Software-Defined Radio using Realtek RTL2832U chipset) is the most common affordable hardware that allows users to receive and process ADS-B messages. There are multiple software options for message decoding (dump1090, RTL1090, SDRSharp) that provide tracking data and map visualizations. To allow reliable readings of ADS-B messages, hardware and software settings have to be appropriately configured. These include configuration of central frequency, sample rate, gain, as well as automatic gain control and noise filtering if allowed by the software.

The central issue in localization based on crowdsourced data is verification of receiver location and time synchronization. It is important to note, that these can not be guaranteed for the majority of non-verified receivers that comprise about 80 percent of all registered receivers in LocaRDS [5]. In theory, RTL-SDR equipment can achieve synchronization accuracy of 100 nanoseconds that corresponds to localization error of 30 meters [20]. In addition to hardware settings and Mode S implementation, the intentional data breaches, software bugs, environmental noise and transponder misconfiguration were identified as potential causes for erroneous measurements received by OpenSky Network [14].

2.4. Localization methods

In general, localization methods can be divided in two groups as shown in figure 2.4. Range-based localization relies on the distance measurements between nodes whereas range-free localization utilizes information about connectivity of the nodes. Range-based localization methods are preferred whenever an accurate distance measurement or estimation is available, as these generally provide higher level of accuracy compared to range-free techniques [21].

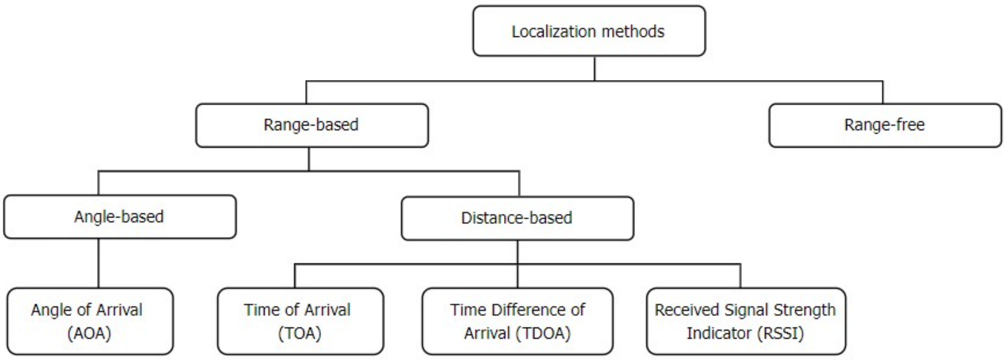

Figure 2.4: Taxonomy of localization methods.

Further division of range-based methods originates from the nature of measurements. AOA provides directional information about the transmitter, but does not directly measure distance. It is usually used in conjunction with other methods due to its limitations in angle ambiguity and range. On the contrary, TOA and TDOA are directly related to the distance, whereas RSS can be related to distance through signal propagation model. In the scope of this thesis, distance-based methods will be further discussed in this section.

2.4.1. TOA/TDOA: Time of Arrival and Time Difference of Arrival

TOA measures the absolute time it takes for signal to travel from transmitter to the receiver, while TDOA measures the time difference of arrival at multiple receiving points. TDOA based methods are usually more accurate compared to ones utilizing TOA [22]. Primarily, errors in both methods arise from the fact the accurate clock synchronization between receivers is problematic. A comparable accuracy of TOA and TDOA methods can be achieved provided time synchronization or elimination of measurements with faulty timestamps [23]. Time for synchronization is usually sourced from GPS that, provided good reception, allows up to 9 nanosecond synchronization in receivers, which in turn corresponds to localization accuracy of 30 meters. GPS time synchronization is limited to LOS propagation between GPS and the receiver and can not be guaranteed during GPS outages. Other options include more sophisticated synchronization methods such as Network Time Protocol (NTP), Precision Time Protocol (PTP) and Pulse-per-Second (PPS) signals [2]. It is important to note, that receivers often require additional hardware for the purpose of time synchronization, which comes at additional cost. While synchronization is usually attributed to as a number one concern in time-based localization, there are other considerations that include sample rate and geometric dilution of precision.

Sample rate set by the receiver is another factor that can influence TDOA localization accuracy. For ADS-B signals, a sample rate of 2.048 Msps is commonly used. Although increasing sample rate comes with finer temporal resolution that allows better measurement of time differences, it also increases computational load and noise impact, as the variations between successive samples become increasingly related to noise rather than to variations in the signal. It was shown that along with frequency content and SNR, the estimation algorithm should also be considered in terms of chosen sample rate [24].

Lastly, TDOA-based localization is dependent on geometric dilution of precision (GDOP) that is a measure of localization error that originates from geometric arrangement of transmitter relative to the receivers. It is computed using positional and timing uncertainties. A low GDOP value indicates low uncertainty that is defined by two factors: the transmitter location and relative position of receivers. The lowest GDOP is achieved when the transmitter is located within the perimeter outlined by receivers as shown in figure 2.5(a) and the localization error increases significantly when the transmitter moves outside this perimeter [3].

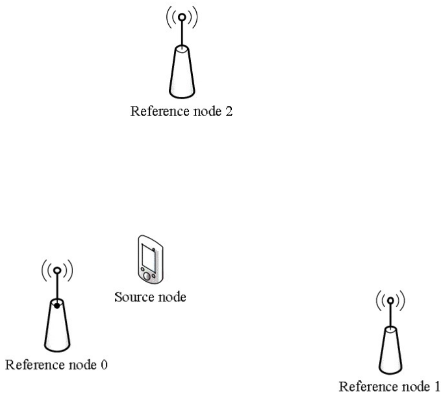

(a) Transmitter within the perimeter outlined by receivers. Adapted from [3].

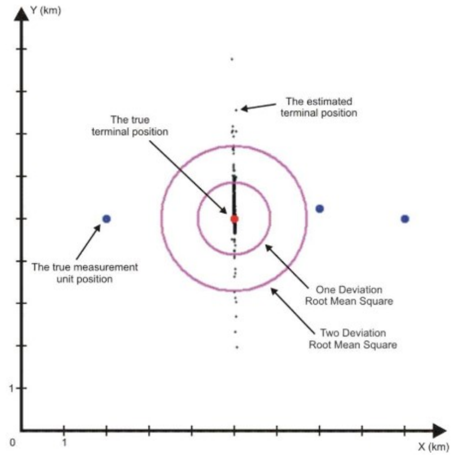

(b) Linear configuration of transmitter and receivers. Adapted from [25].

Figure 2.5: Geometry considerations for TDOA-based localization accuracy.

As for the relative position of receivers, better accuracy is achieved when receivers are spread in a specific manner. In the scenario with three receivers that form a triangle, configuring the receivers in equilateral triangle results in the lowest GDOP, whereas the accuracy decreases when the triangle gets skewed [3]. The critical case of such skewness is linear configuration of transmitter and receivers as shown in figure 2.5(b) that results in high localization errors [25]. Moreover, the localization error increases in line with the time measurement error.

2.4.2. RSSI: Received Signal Strength Indicator

Received signal strength indicator (RSSI) is an indication of the power present in the received signal measured in decibel. The RSS measurements may vary based on the environmental conditions and characteristics of both transmitters and receivers [26]. Factors that influence RSS measurements are:

- Transmitter related factors: antenna characteristics, hardware (signal generators and amplifiers), power output.
- Receiver related factors: receiver sensitivity, antenna characteristics, data processing components (filters, amplifiers), bandwidth configuration.
- Environment related factors: multipath propagation, signal fading, signal interference.

It was shown that RSS variations are present even in an ideal scenario that accounts for equipment and environmental uncertainties [27]. Good practice recommendations include calibration of RSS measurements to overcome offsets in power-to-RSS functions and use of isotropic antennas [28]. It is clear that these recommendations are not applicable in the setting where receiver properties are varying or unknown. Therefore, RSS-based localization in a real environment and using standard receivers was pronounced to be inaccurate [4]. However, what makes RSS an attractive feature for localization purposes is that it does not rely on time measurements, eliminating the need for clock synchronization as well as making it more robust to multipath effect.

2.5. Localization algorithms

In this section, localization algorithms that employ TDOA and RSS measurements are explored. First, a technique for TDOA-based positioning known as multilateration is introduced along with its limitations and applicable algorithms. Then, basic RSSI-based algorithms are presented. Lastly, more advanced algorithms that can potentially combine both methods are discussed.

2.5.1. Multilateration

In multilateration (MLAT), the hyperbolic curves are used to determine the position of the transmitter. The geometry of transmitter-receiver network is illustrated in figure 2.6. Theoretically, MLAT requires at least three receivers to determine the 2D position of an aircraft, while four receivers are needed to resolve it in 3D. However, in most cases the receivers are ground based and do not provide sufficient elevation angle diversity needed to resolve vertical component of GDOP [29]. Therefore, the 2D position is usually derived through MLAT, while the altitude is obtained directly from ADS-B message.

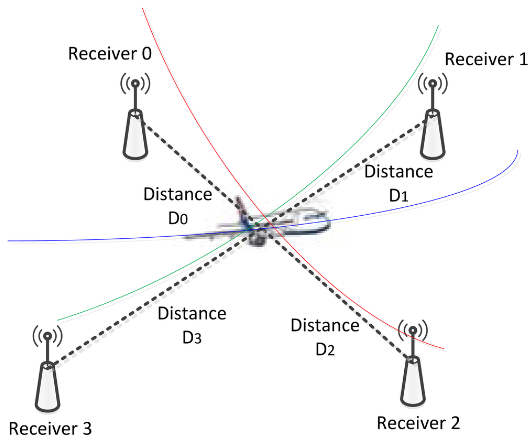

Figure 2.6: Geometry of multilateration. Adapted from [30].

In presence of three receivers, the hyperbolic curves are constructed to satisfy the distances to i^{th}, j^{th} and k^{th} receivers with known coordinates (x_i, y_i, z_i) as given by equations 2.13.

$$\begin{cases} d_i = \sqrt{(x-x_i)^2 + (y-y_i)^2 + (z-z_i)^2} \\ d_j = \sqrt{(x-x_j)^2 + (y-y_j)^2 + (z-z_j)^2} \\ d_k = \sqrt{(x-x_k)^2 + (y-y_k)^2 + (z-z_k)^2} \end{cases} \tag{2.13}$$

These distances are further related to TDOA between pairs of receivers as follows from equations 2.14 with the speed of light c equal to 299792458 m/s.

$$\begin{cases} d_i - d_j = TDOA_{i,j} * c \\ d_j - d_k = TDOA_{j,k} * c \\ d_i - d_k = TDOA_{i,k} * c \end{cases} \tag{2.14}$$

The multilateration equations can be solved for the unknown coordinates of the aircraft (x, y, z) using least squares method with the initial guess being the midpoint of receiver coordinates.

The extended version of MLAT that employs a network of synchronized receivers to cover large geographic areas is known as Wide Area Multilateration (WAM). Such systems provide equivalent or higher level of service compared to traditional secondary surveillance radar (SSR) systems, but the localization accuracy relies on LOS propagation [29]. Also, the accuracy of MLAT is inherited from the limitations of TDOA discussed in the previous chapter. While, in theory, these can be attributed using RSS measurements, the relationship between distance and TDOA is more direct in nature compared to RSS that requires additional modelling thus comes with its own uncertainty. Therefore, time-based methods are preferred for accurate MLAT due to their direct relationship with distance.

2.5.2. RSSI-based algorithms

Using RSS measurements, the distance between transmitter and receiver can be computed using one of the signal propagation models (see chapter 2.2). Knowledge of the distance allows position estimation through direct computation algorithms, such as Min-Max and Weighted Centroid. It should be noted that these algorithms lack localization accuracy due to their simplicity and require measurements from multiple sensors distributed in a specific geometry.

Min-Max

Min-Max algorithm is based on simple geometry, where the bounding square with side length of 2d is drawn around each sensor based on measured RSS. The estimation of transmitter position is then the center of quadrilateral formed by intersection of these squares as shown in figure 2.7. Although Min-Max algorithm offers simplicity and robustness, it is highly sensitive to the geometry of the receivers. It has been shown that receivers have to be placed at the edges of the network and, ideally, be uniformly distributed to overcome considerable errors [31], which might be impractical in large and erratic networks.

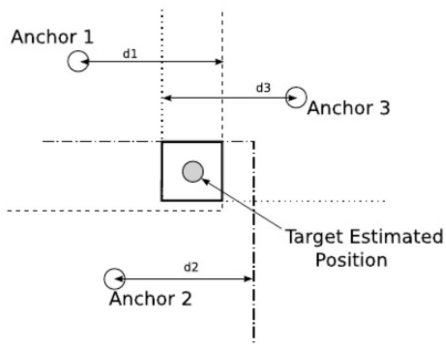

Figure 2.7: The Min-Max algorithm. Adapted from [32].

Weighted Centroid

In Weighted Centroid Localization (WCL) algorithm, each i^{th} receiver is assigned the weight given by the inverse of the distance as $w_i = \frac{1}{d_i}$. The location of the transmitter is then the sum of receiver coordinates multiplied by normalized weight factor W_i. Although, the accuracy of localization increases in line with increasing number of receivers and measurements, the method is prone to high errors primarily due to inaccurate distance estimation by simple signal propagation models [33]. A more sophisticated method, WCL based on Least Square (WCLLS), proposes an additional weighting parameter k that is obtained experimentally and has shown significant localization accuracy improvement in the setting of ten receivers compared to standard WCL algorithm [34].

2.5.3. Advanced RSSI-based algorithms

In this section, advanced RSSI-based algorithms are discussed. In addition to greater localization accuracy, there are theoretical ways to apply these algorithms to TDOA measurements. However, these will not be applicable in the scope of this thesis due to numerous uncertainties, absence of solid background and implementation complexity.

Kalman Filters

Kalman filter (KF) is a recursive algorithm used to estimate the state of the system based on a series of measurements. In localization context, it can be applied for interpolation of corrupted RSS measurements and filtering out the extreme values. The standard KF describes the state x_k and RSS measurements y_k via state transition matrix A that relates a previous state to the current and an observation matrix H. Given observation noises w_k and u_k, the standard KF is of the following form:

$$x_k = A \cdot x_{k-1} + w_k$$

$$y_k = H \cdot x_k + u_k$$

The filtering is done by capturing the predicted dynamics through the signal propagation model of choice and iteratively correcting it based on the observed measurements. The standard KF estimates are significantly more accurate compared to log-distance path loss model especially for low RSS values [35]. It was also shown to be computationally efficient due to its linear nature [36], which in turn highlights its main weakness as it is unable to capture nonlinearities in RSS measurements. In practice, one can overcome this using Extended Kalman Filter (EKF) that linearizes measurement model using Taylor series expansion. However, given perfect knowledge of propagation model, EKF implementation was shown to have minor impact on localization accuracy compared to KF [37].

Linear KF are rarely applied in TDOA-based localization due to the nonlinear relationship between time difference measurements and transmitter position. Prior studies attempted to construct TDOA-based algorithms for nonlinear KF, but these are limited by idealized geometry setting and a small number of receivers [38] or lack of consideration of signal interference effects [39].

Maximum Likelihood

Maximum Likelihood (ML) is an iterative optimization algorithm that aims to find the position that makes the RSS measurements most probable in line with the signal propagation model. By maximizing the likelihood, the algorithm aims to minimize the difference between the expected and measured RSS values. As ML algorithm relies on the number of available RSS measurements, it is prone to high errors with insufficient number of receivers [32]. However, it was found to outperform all direct computation algorithms when the number of receivers is larger than seven [40].

Implementation of ML algorithm with TDOA poses additional difficulties due to the nonlinear nature of time delays when considering synchronization errors. Various authors suggest highly complex solutions that involve integration of frequency difference of arrival (FDOA) [41] or implementation of sophisticated optimization algorithms [42].

Fingerprinting

Fingerprinting relies on creating a database of RSS measuremor fingerprints (off-line phase) and comparing observed RSS values with those stored in the database (on-line phase). This approach offers significantly better positioning accuracy compared to path-loss models alone [43].

In the off-line phase, the training database is usually created using historical data. The size of the training database determines localization accuracy that increases given a greater number of measurements. The trade-off between effort in database collection and localization error is crucial in databases of less than 5000 fingerprints, whereas larger databases offer only minimal improvement in accuracy [44]. For reduction of data collection workload, crowd-sourced fingerprint data can be utilized with consideration of RSS measurement quality [45]. In the on-line phase, matching of observed RSS with fingerprints can be done using machine learning algorithms, such as k-Nearest Neighbours, Support Vector Machines, Gradient Lifting or Logistic Regression. It was shown that all algorithms have comparable performance in terms of positioning accuracy with k-Nearest Neighbours producing slightly more accurate results [44].

Although fingerprinting method mainly relates to RSS-based positioning, the state-of-art research suggests that it can be implemented using TDOA. However, these algorithms require additional data interpolation due to receiver synchronization issues thus making them computationally more complex [46]. It is also not clear whether TDOA fingerprinting localization error is lower compared to TDOA-based multilateration.

Particle Filtering

Particle Filtering (PF), also known as Monte Carlo Localization (MCL), is a probabilistic approach that represents probability distribution of transmitter location using series of weighted samples and constantly updates these samples by prediction and filtering. The algorithm contains five phases, namely: initialization, prediction, weight assignment, resampling and iteration. Whereas the main concern regarding the algorithm addresses the accuracy of prediction, its computational efficiency is addressed in resampling phase.

In the prediction phase, the movement of the particle is described by the motion model. Although many models developed for localization and tracking were described in literature [47], they require better knowledge about the transmitter than is usually available. Also, acceleration and turning characteristics of each moving transmitter can not be accurately captured by a single motion model resulting in biased position estimation [48]. In the resampling phase, a new set of particles is generated to restore the diversity of particles and avoid degeneracy that occurs when a large computational effort is dedicated to update the particles with low weights.

To ensure that particles with higher weights are repeatedly selected, the RSS likelihood can be integrated in the resampling procedure [49]. A more sophisticated MCL Box Localization algorithm [50] showed sampling efficiency improvement through construction of an optimal sampling space. This space is constructed through RSS ranging similarly to the previously discussed Min-Max algorithm.

Similarly to fingerprinting, PF is widely applied as a RSS-based method, but typically not used as TDOA-based approach due to time synchronization issues and nonlinear relationships in signal propagation. Motion models for TDOA-based systems need to consider complex factors such as target velocity and potential geometry changes. However, this complex approach outperforms nonlinear Kalman filters under vast simplifications of motion model [51].

2.5.4. Hybrid algorithms

Various hybrid algorithms were proposed in prior research in order to employ benefits of both TDOA and RSS measurements. As TDOA provides direct geometric information about distances and RSS measurements offer information about the propagation characteristics, a combination of both exploits the accuracy of TDOA while mitigating the impact of environmental variations through RSS. In addition, TDOA methods rely on LOS propagation, while RSS measurements are affected by signal interference and the multipath effect, thus integration of both can lead to more accurate localization in presence of limited LOS. It therefore becomes clear that utilizing both measurements leads to better estimation of position [52].

The hybrid solution can be based on the selection of best distance estimation [53]. While both distances are computed through TDOA estimator and log-normal shadowing model, the latter is selected if measured RSS exceeds a certain threshold. The multilateration equation is then expanded with Gaussian noise and the system can be solved for the unknown position using ML algorithm. Although this approach increases localization accuracy compared to TDOA alone, it is unclear what threshold of selected RSS measurements is suitable for uncontrolled or outdoor environments and whether the algorithm can be applied for longer ranges.

Another uncertainty regarding hybrid algorithms is caused by the lack of studies where system properties such as transmitter and receiver settings are unknown [54]. What is clear, is that the accuracy of hybrid approaches have similar to standard TDOA and RSS-based methods dependency on the number of receivers and their geometry [55].

2.6. Literature review summary

This literature review presented two methods for aircraft localization, namely, TDOA- and RSS-based. Each method was found to have numerous advantages along with the uncertainties that have to be considered in terms of localization accuracy. In this chapter, the advantages and disadvantages of each method are summarized with + and – symbols respectively.

TDOA-based multilateration is characterized by the following:

+ High localization accuracy.

– Relies on LOS propagation, susceptible to multipath effect otherwise.

– Requires time synchronization of receivers.

– Can not resolve vertical component of GDOP (altitude).

The accuracy of RSS-based localization was shown to be strongly dependent on signal propagation mechanisms. These can be captured using signal propagation models. In terms of localization accuracy, RSS-based methods are characterized by the following:

– Strong dependence on signal fading mechanisms and noise.

+ More robust to multipath effect.

– Propagation models are limited to theoretical knowledge of the system.

+ Measurement based propagation models can be derived.

– RSS measurement quality is dependent on transmitter and receiver settings.

+ Does not require additional equipment for receiver synchronization.

In addition, various RSS-based localization algorithms were presented. The accuracy of all algorithms depends on the number of receivers available. It was shown that implementation of more sophisticated algorithms with TDOA is highly complex and it is unclear whether it results in better estimation than with RSS. These algorithms are summarized in table 2.2 in terms of their complexity, accuracy and algorithm-specific requirements.

Table 2.2: Overview of localization methods and algorithms.

Algorithm	**Method**	**Complexity**	**Accuracy**	**Requirements**
Min-Max	RSS	Low	Low	Regular distribution of receivers
Weighted Centroid	RSS	Low	Low	Sophisticated propagation model
Kalman Filters	RSS	High	High	Accurate measurement noise model
	TDOA	Very High	-	-
Maximum Likelihood	RSS	High	High	Sufficient number of receivers
	TDOA	Very High	-	-
Fingerprinting	RSS	High	High	Sufficient size of training database
	TDOA	Very high	-	-
Particle Filtering	RSS	High	High	Accurate motion model
	TDOA	Very high	-	-

3
Research proposal

In this chapter, the contribution of this thesis is described. First, the gap in existing literature and earlier research is established in section 3.1. Consequently, the research objectives are set in section 3.2 in order to minimize the established gap. Lastly, the research questions are formulated and discussed in section 3.3.

3.1. Literature gap

The literature review presented in the previous chapter identified the main challenges of RSS-based localization as strong dependence on signal fading and interference mechanisms as well as on transmitter and receiver quality. It was established that some of these properties can be captured by signal propagation models. However, the state-of-art models focus on limited areas and their performance is evaluated mostly in the setting when the propagation properties are preset or known. In addition, no comparison of localization accuracy between different models was found.

Furthermore, only one study of the crowdsourced data employment for localization purposes was referenced in the literature review. Although it is clear what challenges are faced with RSS-based localization in general, it is yet to be determined how they can be managed in presence of receiver characteristic diversity and biased data collection. This highlights the gap in the existing knowledge of feasibility and implications related to the use of crowdsourced RSS measurements.

3.2. Research objective

The main objective of this research is to determine whether the use of crowdsourced RSS data is feasible in localization context. To fulfill the objective, this thesis will focus on the reliability of the crowdsourced data and applicability of signal propagation models. In addition, the research aims to compare the difference in localization errors between the traditional MLAT technique and RSS-based methods.

3.3. Research questions

In line with the research objective, the central question of this thesis has been formulated as follows:

How can crowdsourced measurements of received signal strength improve the accuracy of aircraft localization?

To answer the main research question, the following sub-questions will be addressed through the actions presented in the flowchart below.

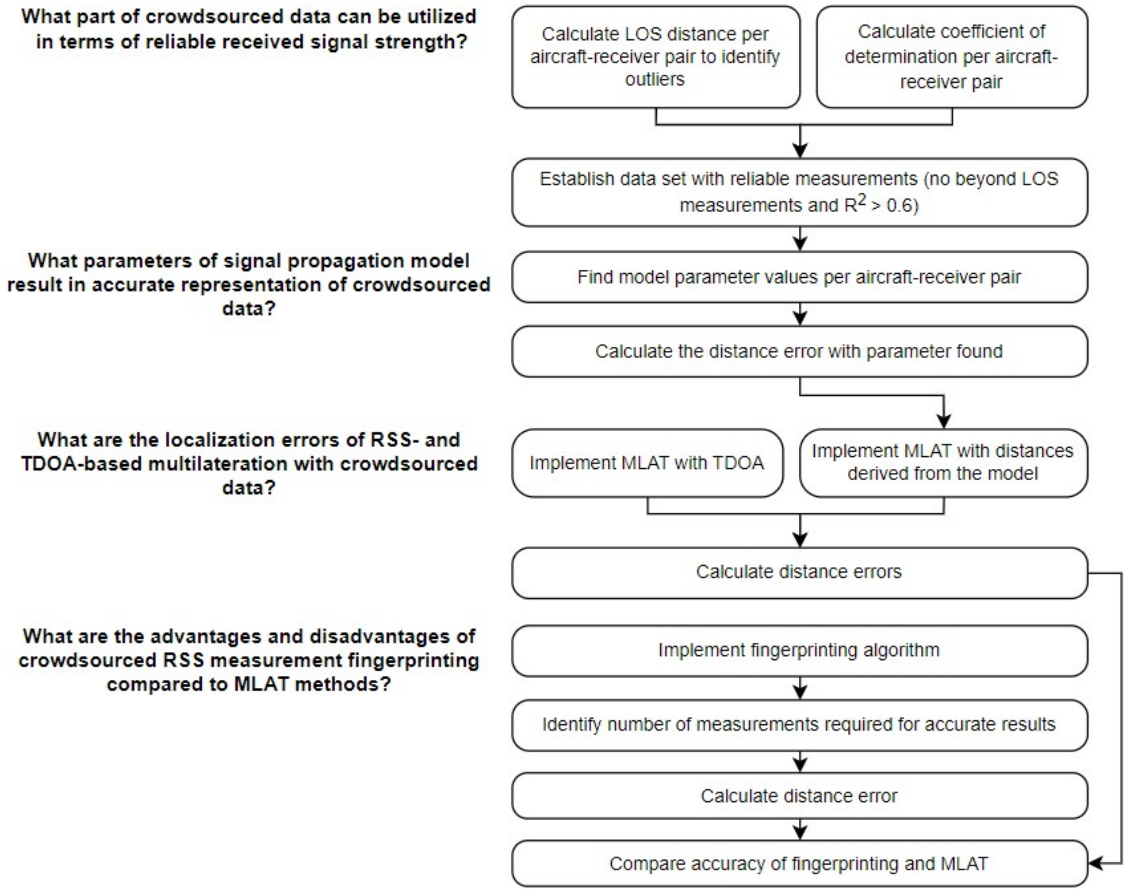

3.4. Planning

The entire work plan for this thesis was divided in three phases: exploratory, implementation and defense. The exploratory phase that includes actions presented under the first research sub-question is completed with the submission of this report. The following implementation phase includes determination of model parameters, MLAT with time and RSS measurements and fingerprinting. In the end of implementation phase, final report will be produced in the form of scientific paper. A full weekly planning of this thesis including the completed activities can be found in Appendix B.

3.5. Data processing

The LocaRDS subset 2 employed in this thesis was retrieved in csv format and consists of 28717685 measurements. Hereby, the methods of data processing employed are discussed.

3.5.1. Outliers

Although the theoretical range of ADS-B transponder can exceed 250 NM or 463 km, it is highly unlikely that a strong signal will be received over such distances. The aircraft-receiver pairs with the separation distances larger than theoretical LOS were identified. In cases where this distance exceeds LOS distance, the measurements are considered to be the outliers and will not be used for further analysis.

3.5.2. Regression models and coefficient of determination

The aim of the regression model is to find the best fitting curve that represents the relationship between variables. To examine this relationship, second order polynomial regression model was constructed for each unique aircraft-receiver pair. In presence of regression model, the coefficient of determination R^2 is computed to examine how well the variability in the distance between the aircraft and the receiver can be explained by the variability in the RSS. The calculation of R^2 is given by equation 3.1 where residual sum of squares (RSS) is given by the squared sum of differences in measured and predicted data, and total sum squares (TSS) is given by the squared sum of differences in measured data and its mean. The R^2 values vary from 0 to 1 where the latter indicates that the regression model perfectly explains the variability in distance based on the variability in RSS.

$$R^2 = 1 - \frac{RSS}{TSS} = 1 - \frac{\sum_{i=1}^{n} (y_i - \hat{y})^2}{\sum_{i=1}^{n} (y_i - \overline{y})^2} \tag{3.1}$$

3.5.3. Implementation phase

The remaining work of this thesis requires to identify the signal propagation model parameters that are representative for the crowdsourced data. This will be done by obtaining parameters for measurement-based propagation model given by equation 2.6. Later, MLAT will be implemented with the time measurements from LocaRDS and the distances obtained through the model. The implementation of MLAT follows from equations 2.13 and 2.14. The localization accuracy will be evaluated using the actual position given by LocaRDS.

The RSS fingerprinting algorithm discussed in the literature study was found to be the most applicable in presence of large data sets. Given the knowledge of exact receiver locations and large set of RSS measurements, the applicability of the algorithm in context of crowdsourced data will be examined and includes the following steps:

1. Random separation of available RSS measurements into observation and test data.
2. Assignment of known positions to RSS measurements in observation data.
3. Matching of observation data and test data by smallest distance.
4. Estimation of position of test data by weighted average of matches.

3.5.4. Software

The programming language used for this thesis is Python. The use of Python 3.11 is facilitated by Anaconda distribution. In context of data processing, the following Python libraries are utilized:

- Pandas: dataset structuring and analysis.
- NumPy: algebraic calculations.
- SciPy: implementation of multilateration.
- Scikit-learn: statistical modeling and machine learning.
- Matplotlib: graphic figure production.

It is likely that other libraries or open source packages will be used throughout this thesis. These might include GeoPandas for spatial data processing and Localization for verification of multilateration results.

3.5.5. Validation of results

The description of entire LocaRDS dataset employed in this thesis can be found in Appendix A. Due to the immense quantity of data points available, it was decided to limit the exploratory phase of this thesis to a single subset in order to minimize the computational load. The initial results were produced from subset 2. Assuming the same quality of data throughout LocaRDS, the results of this thesis can be validated on any other available subset.

4

Preliminary results

Preliminary results of this thesis were obtained using subset 2 of LocaRDS. Due to the considerable size of this data set, the exploratory phase focused on data preprocessing that included establishment of usable data set, elimination of outliers and construction of regression models for each unique aircraft-receiver pair. This chapter presents the preliminary results in sections 4.1 and 4.2 as well as discusses considerations for the remaining work in section 4.3.

4.1. Outliers

Based on the outlier criteria described in research proposal, 36123 outliers were identified. These account for 0.126% of all data points among 203 of total 317 receivers. The distribution between receivers with more than 200 outliers is shown in figure 4.1.

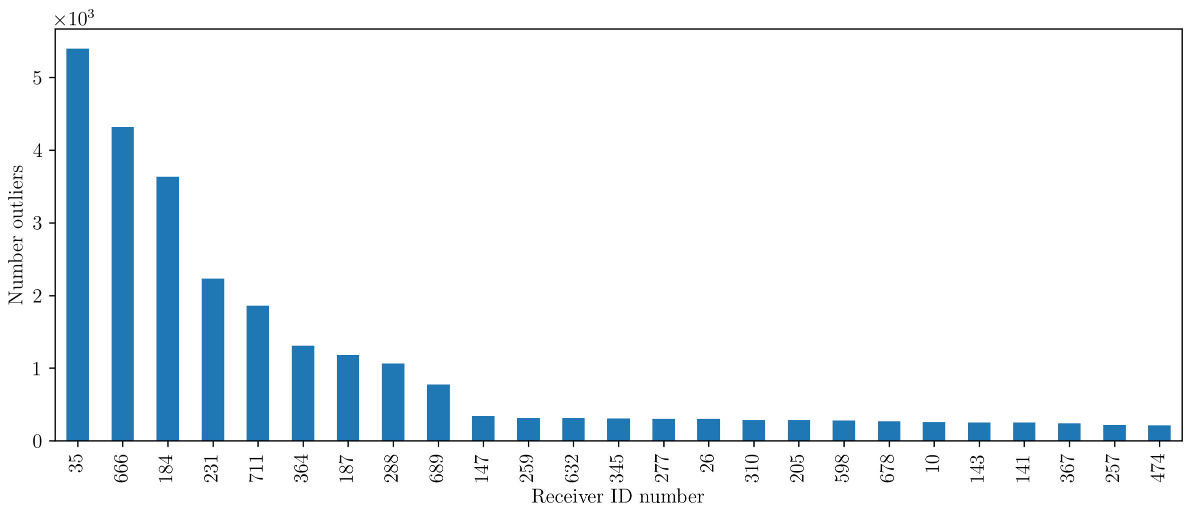

Figure 4.1: Number of outliers per receiver.

The reasons for outlier presence include extended range of the receiver and erroneous measurements. While the latter can be easily spotted as multiple inconsistent measurements at abnormal distances, the transmission range can not be verified. Therefore, the measurements obtained from beyond LOS calculated were not included in the further analysis.

4.2. Regression models

The data set consists of 66942 unique aircraft-receiver pairs. The coefficient of determination R^2 was calculated for each pair. The difference between high and low R^2 values can be observed in figure 4.2, whereas lower value indicates more chaotic distribution of measurements. The threshold of $R^2 > 0.6$ was selected for further analysis.

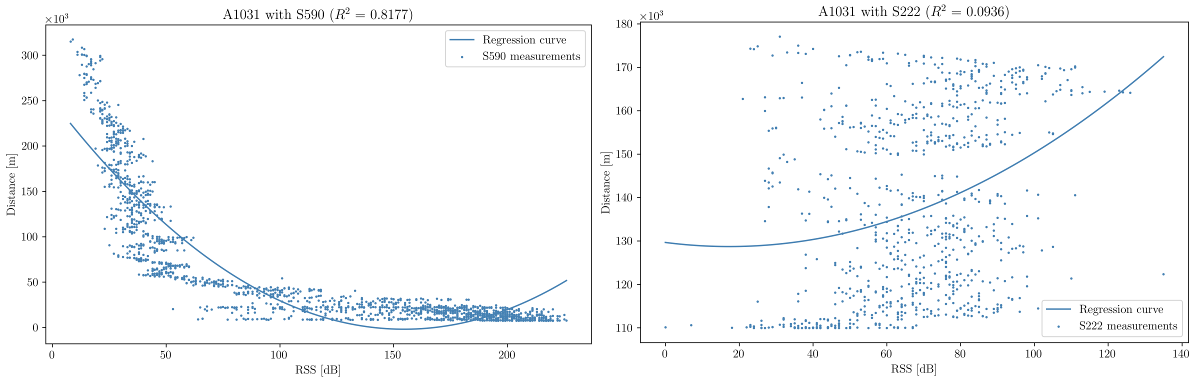

(a) Aircraft 1031 with receiver 590.

(b) Aircraft 1031 with receiver 222.

Figure 4.2: Examples of high and low coefficient of determination R^2 in regression models.

As the transmission power remains relatively constant, the aim was to identify whether there are at least three receivers per aircraft that obtained the signal. In addition, only the pairs with more than 50 available measurements were considered to ensure the proper fit of regression model. These account for 49491 pairs in the data set. With these limitations, 409 aircraft combinations with more than three receivers were found. Based on the criteria, all combinations were found to fall under the following categories:

- Good agreement models: the regression models have similar pattern or overlap.
- Good agreement for combination: the regression models might not have the similar pattern, but are distributed in the manner appropriate for combination.
- Good agreement for parameters: the regression models have similar pattern, but are spread over the distances.
- Poor agreement models: the models are not similar or are distributed in a chaotic manner.

These are discussed further in this section. The models identified under first three categories of good agreement account for 326 out of 409 aircraft-receiver combinations. It should be also noted, that for the majority of the aircraft only three receivers that comply with $R^2 > 0.6$ could be found. The maximum number of receivers to comply with given criteria is nine. With more than three receivers most of the regression models fall under good agreement for combination or good agreement for parameters category.

Good agreement models

The examples of aircraft-receiver combinations that were identified as good agreement models are given in figure 4.3. 69 out of 409 aircraft-receiver combinations were found in this category. These measurement comply with the expectations of signal propagation models which can be directly verified in the implementation phase of this thesis.

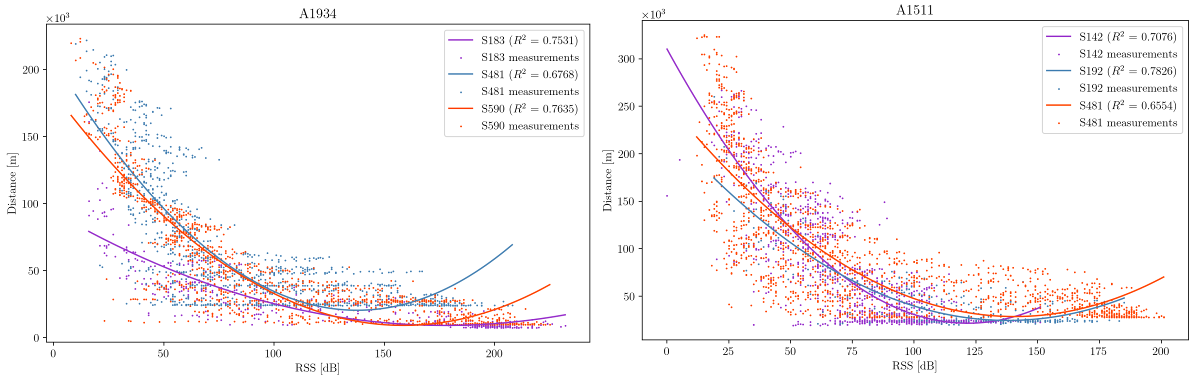

(a) Aircraft 1934.

(b) Aircraft 1511.

Figure 4.3: Examples of regression models with good agreement.

Good agreement for combination

In this category the measurements are limited by the receiver reception range. As can be seen in figure 4.4, the distribution of measurements from various receivers complies with the expectations of signal propagation model similarly to the previous category discussed. It is therefore expected that combination of these measurements provides sufficient accuracy. The total of 100 aircraft-receiver combinations were identified in this category.

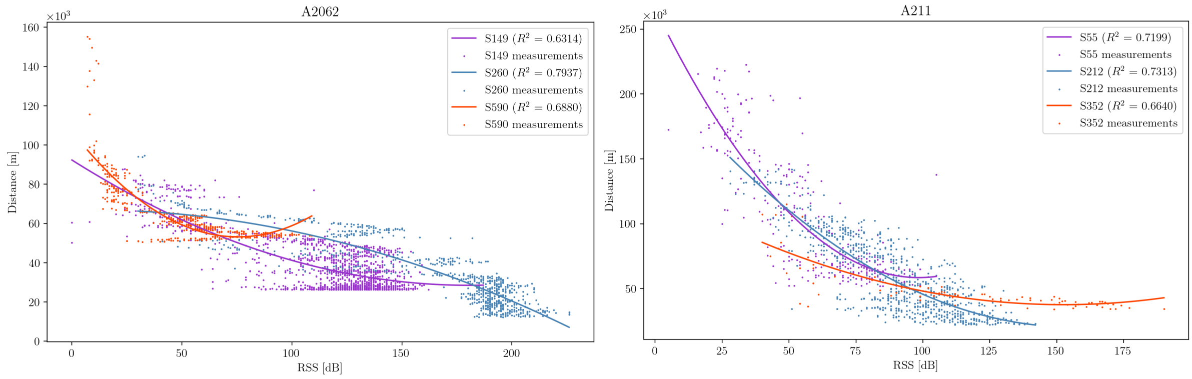

(a) Aircraft 2062.

(b) Aircraft 211.

Figure 4.4: Examples of regression models with good agreement for combination.

Good agreement for parameters

The last category good agreement is comprised by 157 regression model combinations that have similar pattern, but are spread over the distances as shown in figure 4.5. This spread can be attributed to the transmitter and receiver parameters that can be captured by signal propagation models. Although these parameters can be estimated for each individual receiver, this falls outside the scope of this thesis. Therefore, only the measurements that comply with the expected model will be used for the remaining work.

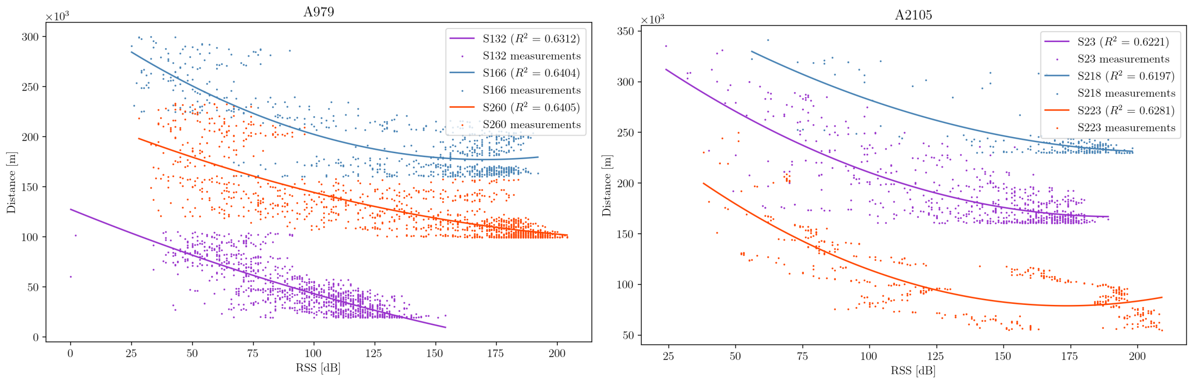

(a) Aircraft 979. **(b)** Aircraft 2015.

Figure 4.5: Examples of regression models with good agreement for parameters.

Poor agreement models

Lastly, the poor agreement models category includes the models that are not similar or are distributed in a chaotic manner. These account for 83 out of 409 aircraft-receiver combinations. The examples of bad fit models are given in figure 4.6. Although it is not entirely clear why such discrepancies between the regression models occur, these can most likely be attributed to the faulty transmitter or receiver. In terms of the remaining work, the aircraft-receiver pairs that were found to have a poor agreement will be discarded.

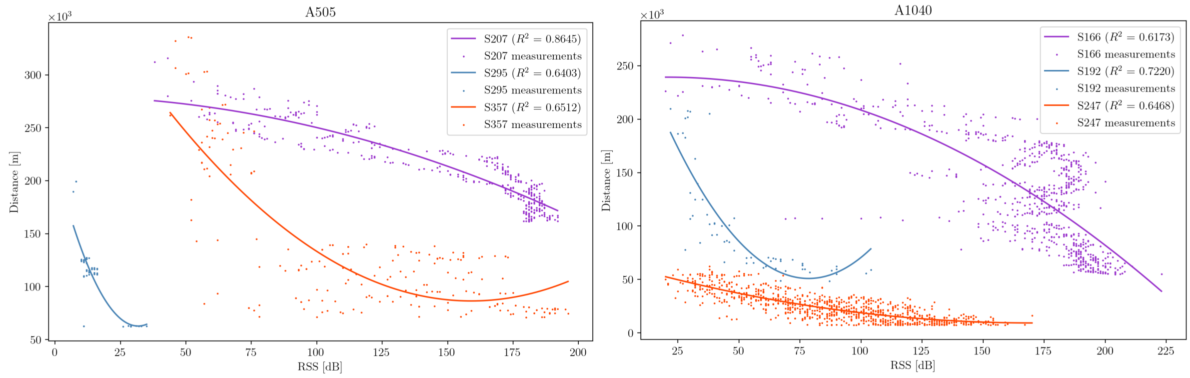

(a) Aircraft 505. **(b)** Aircraft 1040.

Figure 4.6: Examples of regression models with poor agreement.

4.3. Considerations for implementation phase

The remaining work of this thesis includes determination of propagation model parameters, MLAT with time and RSS measurements and fingerprinting. The first two are straightforward and not going to be elaborated further. The consideration for fingerprinting implementation regards the data points available for the construction of training database. From the figures presented in the previous section, it is clear that the message count per sensor varies significantly. Also, some combinations of sensors include little number of RSS measurements. Therefore, it should be later examined whether the training data set contains enough data points for accurate localization based on the available RSS measurements.

The last remark considers two binary indicators of measurement quality, namely, aircraft location and receiver location and synchronization accuracy, provided in LocaRDS data set. No significant difference was observed with respect to these indicators during the exploratory phase. In contrast, various pairs of trusted aircraft and verified receivers produced inconsistent RSS measurements. Therefore, the division in trusted and not trusted receivers and aircraft will no longer be considered for RSS-based calculations.

5
Conclusion

The aircraft localization based on the RSS measurements has not been actively addressed by the state-of-art studies. However, it is clear that use of RSS alleviates MLAT synchronization and geometry-related limitations. It was established that the quality of RSS measurements depends on the transmitter and receiver properties as well as on the environmental factors. Unfortunately, transmitter and receiver properties are unknown in the context of this thesis. However, these can be parameterized by the measurement-based signal propagation model.

The exploratory phase of this thesis addressed the quality of crowdsourced RSS measurement data. It was found that roughly 0.126% of all data was received from the distances that extend beyond LOS. As it is impossible to verify the transmission range for each aircraft-receiver pair, these measurements were not considered in the further analysis. The regression models were constructed for the rest of the data to identify how well the variability in the RSS is explained by the variability in the distance. 409 combinations of one aircraft and at least three receivers were found to comply with the threshold of $R^2 > 0.6$. Out of these, 83 combinations produced the regression models that are not similar in nature or are chaotically distributed. These discrepancies were attributed to the faulty transmitter or receiver. The remaining 326 combinations will be used for further work in this thesis that can be ultimately expanded on the entire data set for validation of results.

The remaining work of this thesis includes determination of model parameters, MLAT with time and RSS measurements and implementation of fingerprinting algorithm. For the latter, it should be further established whether the combinations of aircraft-receiver with good quality measurements have sufficient number of data points to facilitate an accurate RSS fingerprint-based localization.

Bibliography

[1] J. Roudet, P.-E. Thurat, and N. Turcot. Airport Ground-traffic Surveillance Systems Data Feed Innovative Comprehensive Analysis. *Transportation Research Procedia*, vol. 14: pp. 3741–3750, 2016.

[2] D. Chefrour. “Evolution of network time synchronization towards nanoseconds accuracy: A survey”. Computer Communications(191):pp. 26–35, 2022. doi: 10.1016/j.comcom.2022.04.023.

[3] Y. Zhao, C.-H. Lung, I. Lambadaris, and N. Goel. ”Improving location identification in wireless ad hoc/sensor networks using GDOP theory”. 2009 Third International Conference on Sensor Technologies and Applications:pp. 223–228, 2009. doi: 10.1109/SENSORCOMM.2009.44.

[4] K. Heurtefeux and F. Valois. ”Is RSSI a good choice for localization in wireless sensor network?”. 2012 IEEE 26th International Conference on Advanced Information Networking and Applications:pp. 732–739, 2012. doi: 10.1109/AINA.2012.19.

[5] M. Schäfer, M. Strohmeier, M. Leonardi, and V. Lenders. ”LocaRDS: A localization reference data set”. *Sensors*, 21(16):5516, 2021. doi: 10.3390/s21165516.

[6] T.S. Rappaport. *”Wireless Communications: Principles and Practice”*. Prentice Hall PTR, 2nd edition, 2002.

[7] Y. Jang, H. Lim, and D. Yoon. ”Multipath effect on radar detection of nonfluctuating targets”. *IEEE Transactions on Aerospace and Electronic Systems*, vol. 51(1):pp. 792–795, 2015. doi: 10.1109/TAES.2014.130653.

[8] David C. Torney. ”Localization and observability of aircraft via Doppler shifts”. IEEE Transactions on Aerospace and Electronic Systems(43):pp.1163–1168, 2007. doi: 10.1109/TAES.2007.4383606.

[9] Y. Zhao, D. Hu, Y. Zhao, and Z. Liu. ”Moving target localization for multistatic passive radar using delay, doppler and doppler rate measurements”. *Journal of Systems Engineering and Electronics*, vol. 31(5):pp. 939–949, 2020. doi: 10.23919/JSEE.2020.000071.

[10] D. Zhang, W. Xie, Z. Liao, W. Zhu, L. Jiang, and Y. Zou. ”Beyond RSS: A PRR and SNR aided localization system for transceiver-free target in sparse wireless networks”. *IEEE Transactions on Mobile Computing*, 21(11):pp. 3866–3879, 2022. doi: 10.1109/TMC.2021.3063629.

[11] A. Pawlitzki and H. Neufeldt. ”Real time performance monitoring and noise analysis in an operational WAM system”. 2011 Tyrrhenian International Workshop on Digital Communications - Enhanced Surveillance of Aircraft and Vehicles:pp. 207–212, 2011.

[12] S.-H. Fang and Y.-H.S. Yang. ”The impact of weather condition on radio-based distance estimation: A case study in GSM networks with mobile measurements”. IEEE Transactions on Vehicular Technology(8):pp. 6444–6453, 2016. doi: 10.1109/TVT.2015.2479591.

[13] N. Jeftenić, M. Simić, and Z. Stamenković. ”Impact of environmental parameters on SNR and RSS in LoRaWAN”. 2020 International Conference on Electrical, Communication, and Computer Engineering (ICECCE):pp.1–6, 2020. doi: 10.1109/ICECCE49384.2020.9179250.

[14] M. Schäfer, M. Strohmeier, M. Smith, M. Fuchs, V. Lenders, and I. Martinovic. ”OpenSky report 2018: Assessing the integrity of crowdsourced Mode S and ADS-B data”. IEEE/AIAA 37th Digital Avionics Systems Conference (DASC):pp. 1–9, 2018. doi: 10.1109/DASC.2018.8569833.

[15] J. Naganawa, J. Honda, T. Otsuyama, H. Tajima, and H. Miyazaki. ”Evaluating path loss by extended squitter signals for aeronautical surveillance”. IEEE Antennas and Wireless Propagation Letters(16):pp. 1353–1356, 2017. doi: 10.1109/LAWP.2016.2635157.

[16] J. Sun and J.M. Hoekstra. ”Analyzing aircraft surveillance signal quality at the 1090 Megahertz radio frequency”. ICRAT 2020, 2020.

[17] T. Mahmood, H.K. AL-Qaysi, and A.S. Hameed. ”The effect of antenna height on the performance of the okumura/hata model under different environments propagation”. 2021 International Conference on Intelligent Technologies (CONIT):pp. 1–4, 2021. doi: 10.1109/CONIT51480.2021.9498395.

[18] M. Strohmeier, M. Schäfer, V. Lenders, and I. Martinovic. ”Realities and challenges of nextgen air traffic management: the case of ADS-B”. *IEEE Communications Magazine*, vol. 52(5):pp. 111–118, 2014. doi: 10.1109/MCOM.2014.6815901.

[19] D. McCallie, J. Butts, and R. Mills. ”Security analysis of the ADS-B implementation in the next generation air transportation system”. *International Journal of Critical Infrastructure Protection*, vol. 4:pp. 78–87, 2011. doi: 10.1016/j.ijcip.2011.06.001.

[20] A. Li and Y. Zheng. ”Research and implementation of wireless TDOA positioning station synchronization based on RTL-SDR”. 2022 IEEE 6th Information Technology and Mechatronics Engineering Conference (ITOEC)(6):pp. 1087–1090, 2022. doi: 10.1109/ITOEC53115.2022.9734446.

[21] E. Shakshuki, A. Elkhail, I. Nemer, M. Adam, and T. Sheltami. ”Comparative study on range free localization algorithms”. *Procedia Computer Science*, 151:pp. 501–510, 2019. doi: 10.1016/j.procs.2019.04.068.

[22] G. Shen, R. Zetik, and R.S. Thoma. ”Performance comparison of TOA and TDOA based location estimation algorithms in los environment”. 2008 5th Workshop on Positioning, Navigation and Communication:pp. 71–78, 2008. doi: 10.1109/WPNC.2008.4510359.

[23] C. Steffes, W. Konle, and W. Koch. ”TDOA/TOA-based geolocation using ADS-B transponder signals — experimental results”. 2017 Sensor Data Fusion: Trends, Solutions, Applications (SDF):pp. 1–6, 2017. doi: 10.1109/SDF.2017.8126354.

[24] O. El Mountassir, B. G. Stewart, S. G. McMeekin, and A. Ahmadinia. ”Effect of sampling rate on the location accuracy of measurements from radiated RF partial discharges signals”. 2012 11th International Conference on Environment and Electrical Engineering: pp. 891–896, 2012. doi: 10.1109/EEEIC.2012.6221502.

[25] K. Bronk and J. Stefanski. ”Bad geometry influence on positioning accuracy in wireless networks”. EUROCON 2007 - The International Conference on ”Computer as a Tool”:pp. 1131–1135, 2007. doi: 10.1109/EURCON.2007.4400257.

[26] D. Capriglione, L. Ferrigno, E. D’Orazio, V. Paciello, and A. Pietrosanto. ”reliability analysis of RSSI for localization in small scale WSNs”. 2012 IEEE International Instrumentation and Measurement Technology Conference Proceedings:pp. 935–940, 2012. doi: 10.1109/I2MTC.2012.6229301.

[27] K.H.M. Azmi, S.M. Berber, and M.J. Neve. ”The influence of received signal strength measurement methods on the accuracy of distance estimation in wireless sensor network”. 2017 IEEE 4th International Conference on Smart Instrumentation, Measurement and Application (ICSIMA):pp. 1–5, 2017. doi: 10.1109/ICSIMA.2017.8312011.

[28] A. Zanella. ”Best practice in RSS measurements and ranging”. *IEEE Communications Surveys & Tutorials*, vol.18(4):pp. 2662–2686, 2016. doi: 10.1109/COMST.2016.2553452.

[29] G. Galati, M. Leonardi, P. Magaro, and V. Paciucci. ”Wide area surveillance using SSR mode S multilateration: advantages and limitations”. European Radar Conference, 2005. EURAD 2005.:pp. 225–229, 2005. doi: 10.1109/EURAD.2005.1605606.

[30] T. Cho, C. Lee, and S. Choi. ”Multi-sensor fusion with interacting multiple model filter for improved aircraft position accuracy”. *Sensors*, vol. 13:pp. 4122–4137, 2013. doi: 10.3390/s130404122.

[31] K. Langendoen and N. Reijers. ”Distributed localization in wireless sensor networks: a quantitative comparison”. *Computer Networks*, 43:pp. 499–518, 2003. doi: 10.1016/S1389-1286(03)00356-6.

[32] E. Goldoni, A. Savioli, M. Risi, and P. Gamba. ”Experimental analysis of RSSI-based indoor localization with IEEE 802.15.4”. pages pp. 71–77, 2010. doi: 10.1109/EW.2010.5483396.

[33] J.D. Sretenović, S.M. Kostić, and M.I. Simić. ”Experimental analysis of weight-compensated weighted centroid localization algorithm based on RSSI”. 2015 12th International Conference on Telecommunication in Modern Satellite, Cable and Broadcasting Services (TELSIKS):pp. 373–376, 2015. doi: 10.1109/TELSKS.2015.7357834.

[34] S. Xie, Y. Hu, and Y. Wang. ”Weighted centroid localization algorithm based on least square for wireless sensor networks”. 2014 IEEE International Conference on Consumer Electronics - China:pp. 1–4, 2014. doi: 10.1109/ICCE-China.2014.7029867.

[35] A. Abusara and M. Hassan. ”Error reduction in distance estimation of RSS propagation models using Kalman filters”. 2015 6th International Conference on Modeling, Simulation, and Applied Optimization (ICMSAO):pp. 1–5, 2015. doi: 10.1109/ICMSAO.2015.7152239.

[36] J.G. Markoulidakis, C. Desiniotis, and D. Nikolaidis. ”Stamp accuracy enhancement through received signal strength adaptive Kalman filtering”. 2007 IEEE 18th International Symposium on Personal, Indoor and Mobile Radio Communications:pp. 1–5, 2007. doi: 10.1109/PIMRC.2007.4394031.

[37] M. Page and T.L. Wickramarathne. ”Enhanced situational awareness with signals of opportunity: RSS-based localization and tracking”. 2019 IEEE Intelligent Transportation Systems Conference (ITSC):pp. 3833–3838, 2019. doi: 10.1109/ITSC.2019.8917116.

[38] Chen H., Deng P., Xu Y., and Li X. ”A robust location algorithm with biased extended kalman filtering of TDOA data for wireless sensor networks”. 2005 International Conference on Wireless Communications, Networking and Mobile Computing, 2005.(2):pp. 883–886, 2005. doi: 10.1109/WCNM.2005.1544192.

[39] C.O. Savage, R.L. Cramer, and H.A. Schmitt. ”TDOA geolocation with the unscented kalman filter”. 2006 IEEE International Conference on Networking, Sensing and Control: pp. 602–606, 2006. doi: 10.1109/ICNSC.2006.1673214.

[40] G. Zanca, F. Zorzi, A. Zanella, and M. Zorzi. ”Experimental comparison of RSSI-based localization algorithms for indoor wireless sensor networks”. 2008. doi: 10.1145/1435473.1435475.

[41] H. Yu, G. Huang, J. Gao, and Wu X. ”Approximate maximum likelihood algorithm for moving source localization using TDOA and FDOA measurements”. *Chinese Journal of Aeronautics*, vol. 25:pp. 593–597, 2012. doi: 10.1016/S1000-9361(11)60423-8.

[42] X. Ma, T. Ballal, H. Chen, O. Aldayel, and T.Y. Al-Naffouri. ”A maximum-likelihood TDOA localization algorithm using difference-of-convex programming”. IEEE Signal Processing Letters(28):pp. 309–313, 2021. doi: 10.1109/LSP.2021.3051836.

[43] N.A.M. Maung and W. Zaw. ”Comparative study of RSS-based indoor positioning techniques on two different wi-fi frequency bands”. 2020 17th International Conference on Electrical Engineering/Electronics, Computer, Telecommunications and Information Technology (ECTI-CON):pp. 185–188, 2020. doi: 10.1109/ECTI-CON49241.2020.9158211.

[44] X. Han and Z. He. ”A wireless fingerprint location method based on target tracking”. 2018 12th International Symposium on Antennas, Propagation and EM Theory (ISAPE): pp. 1–4, 2018. doi: 10.1109/ISAPE.2018.8634177.

[45] C.L. Leca, P. Ciotirnae, C.I. Rincu, and I. Nicolaescu. ”Characteristics of crowdsourcing for outdoor radio fingerprinting positioning”. 2017 9th International Conference on Electronics, Computers and Artificial Intelligence (ECAI):pp. 1–4, 2017. doi: 10.1109/ECAI.2017.8166385.

[46] G. Ouyang, T. Qi, L. Wei, and B. Wang. ”Indoor localization based on sparse TDOA fingerprints”. 2022 IEEE 25th International Conference on Computational Science and Engineering (CSE):pp. 1–8, 2022. doi: 10.1109/CSE57773.2022.00010.

[47] X. Rong Li and V.P. Jilkov. ”survey of maneuvering target tracking. part i. dynamic models”. IEEE Transactions on Aerospace and Electronic Systems(4):pp. 1333–1364, 2003. doi: 10.1109/TAES.2003.1261132.

[48] H. Lu, S. Zhang, X. Liu, and X. Lin. ”Vehicle tracking using particle filter in Wi-Fi network”. 2010 IEEE 72nd Vehicular Technology Conference - Fall:pp. 1–5, 2010. doi: 10.1109/VETECF.2010.5594099.

[49] Q. Shao, H. Xu, L. Jia, and P. Li. ”The research of Monte Carlo localization algorithm based on received signal strength”. 2011 7th International Conference on Wireless Communications, Networking and Mobile Computing:pp. 1–4, 2011. doi: 10.1109/wicom.2011.6040126.

[50] G. Li, J. Zhang, J. Chen, and Z. Xu. ”A Monte Carlo box localization algorithm based on RSSI”. Proceedings of the 33rd Chinese Control Conference:pp. 395–400, 2014. doi: 10.1109/ChiCC.2014.6896655.

[51] R.M. Shubair and H. Elayan. ”Enhanced WSN localization of moving nodes using a robust hybrid tdoa-pf approach”. 2015 11th International Conference on Innovations in Information Technology (IIT):pp. 122–127, 2015. doi: 10.1109/INNOVATIONS.2015.7381526.

[52] M. Laaraiedh, L. Yu, S. Avrillon, and B. Uguen. ”Comparison of hybrid localization schemes using RSSI, TOA, and TDOA”. 17th European Wireless 2011 - Sustainable Wireless Technologies:pp. 1–5, 2011.

[53] S. Tiwari, R. Darraji, S. A. Bassam, A. Kwan, K. Rawat, M. Rawat, M. Fattouche, and F. M. Ghannouchi. ”Practical result of wireless indoor position estimation by using hybrid TDOA/RSS algorithm”. CCECE 2010:pp. 1–5, 2010. doi: 10.1109/CCECE.2010.5575134.

[54] M. Hedley and Q. Zhai. ”Wireless sensor network using hybrid TDOA/RSS tracking of uncooperative targets”. 2014 International Symposium on Wireless Personal Multimedia Communications (WPMC):pp. 385–390, 2014. doi: 10.1109/WPMC.2014.7014849.

[55] I.O. Tovkach, S.Y. Zhuk, O.S. Neuimin, and V.O. Chmelov. ”Analysis of influence of number of sensors on accuracy of radio source position determination based on TDOA-, RSS- and AOA- measurements”. 2021 IEEE 3rd Ukraine Conference on Electrical and Computer Engineering (UKRCON):pp.217–220, 2021. doi: 10.1109/UKRCON53503.2021.9575365.

A

LocaRDS data content

LocaRDS dataset consists of eight subsets, each containing one hour of data. In each subset (see table A.1), numerous locations reported by ADS-B were verified based on the timestamps provided by GPS-synchronized receivers.

Subset	Data point count	Verified count	Receiver count	GPS
1	28234130	1839760	318	45
2	28717685	1680956	317	45
3	28749671	1996987	318	44
4	28215712	1810382	317	43
5	26313445	1452447	314	41
6	27360671	540953	313	40
7	27514781	779524	313	39
8	27395507	1793618	309	42

Table A.1: LocaRDS data set attributes. Adapted from [5].

Each data point is contains the following information:

- Aircraft location: latitude and longitude (WGS84 coordinates in decimal degrees), barometric altitude (in meters), geometric altitude (in meters).
- Receiver location: latitude and longitude (WGS84 coordinates in decimal degrees), height (in meters).
- Receiver timestamp: time measured by the receiver since the beginning of recording at the time of signal arrival (in nanoseconds).
- Server timestamp: time measured by the server since the beginning of recording at the time when ADS-B position report was first observed (in seconds).
- Received signal strength: signal strength measured by the sensor (in decibel).

In addition, two binary indicators are provided:

- Aircraft location accuracy: location is known to have high quality (true), location is known to have low quality (false), aircraft could not be verified (no indicator).
- Receiver location and synchronization accuracy: provided time stamp did not drift during one hour of measurements and receiver location could be verified (true), otherwise (no indicator).

B
Planning

		Week 1	Week 2	Week 3	Week 4
Exploratory phase	April	Establish the topic	Establish research goals and questions	Sort data into processable dataset	Determine RSS/ distance relationship
	May	Literature review	Literature review	Literature review	Sort data per receiver/ per sensor
	June	Analyze the outliers	Regression models for all unique pairs	Downsample data and regression models	Find combinations with at least 3 sensors
	July	Establish final usable dataset	Analyze the results	Write the preliminary report	Write the preliminary report
Implementation phase	August	Write the preliminary report	Finalize and hand in the preliminary report	Adjust the preliminary report	Compute propagation models
	September	Examine model parameters	MLAT with TDOA	MLAT with model predicted distances	Holiday
	October	Holiday	Holiday	Comparison of results	Fingerprinting
	November	Fingerprinting	Fingerprinting	Comparison of results	Analysis of all findings
	December	Write the report	Write the report	Hand in the draft report / green light	Holiday
Defense	January	Adjust the report	Hand in the final report	Prepare the presentation	Prepare the presentation
	February	Defense			

Figure B.1: Weekly planning (completed activities shaded in blue).